Title: Fear conditioning biases olfactory sensory neuron frequencies across generations

Authors: Clara W. Liff [4,1], Yasmine R. Ayman[1], Eliza C.B. Jaeger[1], Avery Cardeiro[1], Hudson S. Lee[1], Alexis Kim[1], Angélica V. Albarracín[1], Dianne-Lee K.D. Ferguson[1,2], Bianca J. Marlin[1,2,3,4]*

Affiliations:

[1]Mortimer B. Zuckerman Mind Brain and Behavior Institute, Columbia University; New York, 10027, USA.

[2]Howard Hughes Medical Institute, Columbia University, New York, NY, USA.

[3]Department of Psychology, Columbia University; New York, 10032, USA.

[4]Department of Neuroscience, Columbia University; New York, 10032, USA.

*Corresponding author. Email: bjm2174@columbia.edu

Abstract: The main olfactory epithelium initiates the process of odor encoding. Recent studies have demonstrated intergenerationally inherited changes in the olfactory system in response to fear conditioning, resulting in increases in olfactory sensory neuron frequencies and altered responses to odors. We investigated changes in the cellular composition of the olfactory epithelium in response to an aversive stimulus. Here, we achieve volumetric cellular resolution to demonstrate that olfactory fear conditioning increases the number of odor-encoding neurons in mice that experience odor-shock conditioning (F0), *as well as their unconditioned offspring* (F1). We demonstrate that the increase in F0 is due, in part, to the biasing of the stem cell layer of the main olfactory epithelium. Detailed analysis of F1 behavior revealed subtle odor-specific differences between the offspring of unconditioned and conditioned parents, despite the absence of an active aversion to the conditioned odor. Thus, we reveal intergenerational regulation of olfactory epithelium composition in response to olfactory fear conditioning, providing insight into the heritability of acquired phenotypes.

One-Sentence Summary: Olfactory fear conditioning induces heritable changes to the mouse olfactory system and biases neurogenesis and behavior in both parent and offspring.

Main Text:

Olfactory fear conditioning in mice results in the persistent avoidance of the conditioned odor. Moreover, the number of olfactory sensory neurons (OSNs) that respond to the conditioned odor increases in the main olfactory epithelium (Jones et al. 2008). Strikingly, this increase in the number of specific sensory neurons is observed not only in conditioned F0 males, but also in their unconditioned offspring (F1), despite never having been exposed to the conditioned odor (Dias and Ressler 2014; Aoued et al. 2019; 2020). This phenomenon of intergenerational epigenetic inheritance describes the transfer of information from one generation to the next without alterations to the sequence of the genome.

Transgenerational epigenetic inheritance, the transfer of information beyond the F1 generation, is responsible for several examples of non-Mendelian transmission in plants, fission yeast, and worms (Greer et al. 2011; Schmitz et al. 2011; Rechavi et al. 2014; Yu et al. 2018; Moore et al. 2021). In these organisms, molecular genetics has provided a detailed mechanistic understanding of the transmission of epigenetic information from parent to multiple generations of offspring (Rando and Verstrepen 2007; Fitz-James and Cavalli 2022). While the existence of transgenerational epigenetic inheritance in mammals remains controversial, many studies have demonstrated the intergenerational inheritance of phenotypes in mice (Carone et al. 2010; Dietz et al. 2011; Dias and Ressler 2014; Gapp et al. 2014; Huypens et al. 2016; Q. Chen et al. 2016; Chan et al. 2020; Cunningham et al. 2021; Toussaint et al. 2022). As mice rely heavily on their sense of smell, olfactory conditioning in a parent may provide future generations with an adaptive advantage: enhanced sensitivity to aversive sensory features in the parent's environment. The intergenerational inheritance of olfactory properties provides a tractable model for understanding mammalian epigenetic inheritance because we can ask how signals responsible for specific changes in the nose are transmitted to the gamete, and then to the offspring.

The mechanisms responsible for the intergenerational increase in odor-responsive OSN number following aversive conditioning are more readily addressed in the olfactory epithelium of F0 mice than in F1 progeny. Elucidation of these local signaling events may then provide insight into the more distant transmission of information to the gametes. The mature olfactory sensory epithelium undergoes constant neurogenesis throughout the life of vertebrates. In mice, the lifespan of a mature OSN is estimated to be 30 days, and new sensory neurons are continually generated by the division of basal stem cells and differentiation into mature OSNs (Liberia et al. 2019). Continuous neurogenesis suggests that increases in specific OSN populations following olfactory fear conditioning could result from the increased birth or enhanced survival rate of a specific OSN subtype.

Olfactory perception is initiated by the recognition of odors by a large repertoire of receptors in the MOE. In mice, each mature OSN expresses only one of 1,400 olfactory receptor genes (Buck and Axel 1991). A cell's receptor choice is semi-stochastic and is mediated by a unique mechanism of transactivation that delivers the necessary transcription factors to only one allele of a single receptor gene (Chess et al. 1994; Shykind et al. 2004; Lomvardas et al. 2006). Neurons expressing a given receptor are distributed within a spatially restricted region of the MOE and project with precision to spatially invariant glomeruli in the olfactory bulb. Each odor can interact with multiple distinct receptors, resulting in the activation of a unique ensemble of glomeruli. The recognition of an odor requires the integration of information passed from glomeruli to mitral and tufted cells in the olfactory bulb, and then to convergent downstream olfactory areas (Price and Powell 1970; Price 1985; C.-F. F. Chen et al. 2014; Diodato et al. 2016). If the receptor choice in a developing OSN can be biased by salient odor associations in the environment, this would afford a mechanism to alter OSN frequencies in the MOE, and potentially the subsequent downstream encoding of the odor.

In this study, we performed quantification of OSNs after olfactory fear conditioning, corroborating the results of an increase in the OSNs responsive to the conditioned odor. Moreover, enhanced numbers of these specific OSNs are also observed in the F1 offspring of conditioned fathers. Additionally, we demonstrate that this increase in the F0 generation is

specific to OSN subtypes expressing receptors that respond to the conditioned odor and not a global increase in OSN number. We further demonstrate that a biased increase in specific OSNs after learning is likely to result from the enhanced proliferation of specific OSNs, suggesting that biased receptor choice underlies this phenomenon in the parent and is epigenetically inherited by their offspring. Behavioral analysis of conditioned F0 mice at multiple timepoints revealed avoidance at day 21 but not 42 or 63, despite the persistence of an increase in the number of OSNs responsive to the conditioned odor. Similarly, the F1 offspring of conditioned F0 males exhibited an increase in the number of conditioned odor-responsive OSNs but did not demonstrate an active avoidance of the conditioned odor. However, in-depth behavioral analysis revealed odor-specific effects in F1 cohorts in which offspring of paired F0 males exhibit alterations in behavior in the context of their father's conditioned odor. Ultimately, our findings suggest that heritable increases in OSN populations, although distinct from active avoidance behavior, may influence more nuanced behaviors.

Olfactory fear conditioning leads to an increase in conditioned odor-responsive cells in parents (F0)

In initial experiments, we asked whether we could observe changes in the abundance of receptors responsive to an odor after olfactory fear conditioning. The olfactory receptor M71 responds to the odor acetophenone, whereas the receptor MOR23 responds to the odor lyral (Touhara et al. 1999b; Bozza et al. 2002). Transgenic mice with targeted mutations at the M71 or MOR23 locus to express green fluorescent protein (GFP) allowed for determination of M71 and MOR23 OSN abundance. Male and female Olfr151-IRES-tauGFP$^{+/+}$ (M71-GFP) or Olfr16-IRES-tauGFP$^{+/+}$ (MOR23-GFP) mice were subjected to an aversive olfactory conditioning paradigm in which a 10-second presentation of the odor acetophenone or lyral was paired with 0.75mA foot shock, 5 times daily for 3 consecutive days (Fig. 1B, C.). The unpaired control group received the same number of odor presentations but experienced a 60-second delay between odor presentation and foot shock (Fig. 1C.), while the naïve control group received no conditioning. The MOEs of conditioned mice were surgically extracted 21 days after the initiation of conditioning and subjected to iDISCO+ optical tissue clearing to visualize M71- and MOR23-expressing OSNs in intact olfactory epithelia (Fig. 1B, D, E.) (Renier et al. 2016). Next, we imaged the anterior region of cleared epithelia using light sheet microscopy and counted the number of M71 or MOR23 OSNs in a fixed volume of tissue using automated spot detection software (Fig. 1G, I., Movies S2-S7.).

Importantly, both M71 and MOR23 OSNs are expressed in the same anterior region of the MOE, enabling consistent imaging and counting protocols for both OSN populations. Male and female M71-GFP mice paired with acetophenone exhibited a 33% increase in the number of M71 OSNs 21 days after the initiation of conditioning when compared to unpaired controls (Fig. 1H, S1A. One-way ANOVA. $P<0.0001$. Tukey's multiple comparisons. Naïve vs. F0 paired $P<0.0001$. F0 unpaired vs. F0 paired $P<0.0001$. n=12,11,12.). Male and female MOR23-GFP mice conditioned with lyral exhibited a 39% increase in MOR23 OSNs when compared to unpaired controls (Fig. 1J, S1B. One-way ANOVA. $P<0.0001$. Tukey's multiple comparisons. Naïve vs. F0 paired $P<0.0001$. F0 unpaired vs. F0 paired $P<0.0001$. n=7,9,9.). These results corroborate previous studies and demonstrate that odor-shock pairing leads to an increase in OSN populations that respond to the conditioning odor.

Fear conditioning-induced increases in conditioned odor-responsive cells are heritable (F1)

We next asked whether the increase in the number of odor-responsive OSNs following conditioning is inherited by naïve offspring of conditioned male mice. Ten days after the initiation of conditioning, we bred F0 males from both the unpaired and paired groups with naïve female mice of matching genotypes (M71-GFP$^{+/+}$ or MOR23-GFP$^{+/+}$). Each mating pair was separated ten days after co-housing to ensure that the offspring were never exposed to the conditioned father. Thus, any observed differences in the offspring could be attributed to the contents of the F0 male's germline. We collected and optically cleared MOEs from male and female 8- to 10-week-old F1 offspring and compared the abundance of M71 or MOR23 OSNs. These F1 mice were never exposed to acetophenone or lyral, nor had they undergone olfactory fear conditioning. Nonetheless, we observed a 36% increase in M71 OSNs in male and female F1 mice from fathers that underwent paired fear conditioning with acetophenone (Fig. 1H, S1A, S2A. Tukey's multiple comparisons. F1 unpaired vs. F1 paired P<0.0001. n=12,14.). A similar relative increase of 27% was observed in MOR23 OSNs in male and female F1 mice from fathers that underwent paired fear conditioning with lyral (Fig. 1J, S1B, S2B. Tukey's multiple comparisons. F1 unpaired vs. F1 paired P=0.0002. n=6,6.). These results demonstrate the intergenerational epigenetic inheritance of an olfactory phenotype, namely an increase in specific OSNs in naïve F1 offspring following aversive conditioning in F0.

Increased OSN abundance is specific to OSN subtypes responsive to the conditioned odor

In order to understand how a parental phenotype can be transmitted intergenerationally to future offspring, we decided to first focus on the mechanism underlying the parental phenotype, as it may serve as the basis for the intergenerational mechanism. To investigate the increase in cell number in the parental generation (F0), we first performed a series of control experiments to demonstrate that fear conditioning does not simply lead to a global increase in the number of OSNs in the MOE. First, we took advantage of the fact that the odor propanol does not activate M71 OSNs (Jones et al. 2008; Johnson and Leon 2000). We repeated the same olfactory conditioning paradigm with M71-GFP mice, except with propanol as the conditioned odor, and counted the number of M71 OSNs in iDISCO-cleared intact MOEs (Fig. 2A.). We observed no difference in the number of M71 OSNs between the two groups of mice, indicating that an increase in OSN subtype depends on the conditioned odor activating that OSN population (Fig. 2D. Student's unpaired t-test. Unpaired vs. paired P=0.3009. n=6,7.).

Next, we generated a transgenic mouse line that expresses a tau-fused red fluorescent protein (RFP) in OSNs that express the M71 olfactory receptor (Fig. 2B.). To generate mice with an internal control, we crossed M71-IRES-tauRFP (M71-RFP) mice with MOR23-GFP mice to generate an M71-RFP$^{+/+}$;MOR23-GFP$^{+/+}$ line in which all M71 OSNs are labeled red and all MOR23 OSNs are labeled green (Fig. 2C.). We conditioned these mice with acetophenone and counted the ratio of M71 OSNs to MOR23 OSNs in serial MOE sections. If olfactory fear conditioning leads to a global increase in the number of OSNs in the MOE, we would expect the ratio of M71 to MOR23 OSNs to remain unchanged following conditioning. However, we observed a significant increase in the ratio of M71 to MOR23 OSNs in paired mice only, demonstrating that odor-shock pairing increased the abundance of M71 OSNs relative to a population that does not respond to the conditioned odor (Fig. 2E. One-way ANOVA. P=0.0062. Tukey's multiple comparisons. Naïve vs. paired P=0.0097. Unpaired vs. paired P=0.0163.

n=2,4,4.). Taken together, these experiments indicate that olfactory fear conditioning results in a *specific* increase in the number of cells responsive to the conditioned odor.

Olfactory fear conditioning biases olfactory receptor choice toward conditioned-odor-responsive cell-specific identities

The olfactory epithelium exhibits continuous neurogenesis in mice. This constant turnover of OSNs suggests a possible mechanism for the increase in specific OSN populations responsive to the conditioned odor. The increase in M71 and MOR23 cells following odor-shock pairing could result from a biased increase in either the birth or survival rate of specific OSN subtypes. In initial experiments, we examined the relative number of M71 and MOR23 OSNs born during and immediately after olfactory fear conditioning. We injected M71-GFP and MOR23-GFP mice intraperitoneally with 5-Ethynyl-2′-deoxyuridine (EdU), a thymidine analog that incorporates into newly synthesized DNA and labels newborn cells, during each of the 3 days of training and for 2 subsequent days (Fig. 3A.). On day 21, we quantified the number of EdU-labeled M71 and MOR23 OSNs in MOE sections (Fig. 3A.). Since EdU has a half-life of approximately 35 minutes (Cheraghali et al. 1995), analysis of EdU 16 days after the cessation of injections reflects a pulse-chase, allowing us to quantify a subset of the neurons born during and 2 days following olfactory fear conditioning (Fig. 3B.).

The number of newborn M71 cells (EdU-labeled) out of total M71 cells was 1.24% ± 0.29 in naïve mice, 2.91% ± 0.56 in acetophenone-unpaired mice, and 7.61% ± 0.53 in acetophenone-paired mice (Fig. 3D. One-way ANOVA. P<0.0001. Tukey's multiple comparisons. Naïve vs. paired P<0.0001. Unpaired vs. paired P<0.0001. n=6,6,6.). When lyral was used as the conditioned odor, the number of newborn (EdU-labeled) MOR23 cells out of total MOR23 cells was 0.29% ± 0.06 in naïve mice, 0.55% ± 0.09 in lyral-unpaired mice, and 1.11% ± 0.21 in lyral-paired mice (Fig. 3E. One-way ANOVA. P=0.0120. Tukey's multiple comparisons. Naïve vs. paired P=0.0154. Unpaired vs. paired P=0.0653. n=4,6,8.). For both conditioning odors, we observed a significant increase in the number of newborn odor-responsive OSNs in mice that underwent paired conditioning (Fig. 3D, E.). These observations demonstrate that olfactory fear conditioning with acetophenone and lyral results in a significant increase in the number of newborn M71 and MOR23 cells, respectively. Despite subtype-specific differences in proliferation rates, odor-shock pairing significantly increased the number of newborn cells differentiating into an OSN subtype that responds to the conditioned odor.

Conditioned-odor-responsive cell increase, but not avoidance behavior, is sustained through at least 9 weeks of cell turnover

We observe an increase in M71 OSNs 21 days after the start of acetophenone-paired olfactory fear conditioning. Given the continuous regeneration of the MOE, we next asked if this increase persists at later time points (Fig. 2A.). Since the half-life of the mouse MOE (the amount of time required for half of the epithelium to regenerate) is approximately 26 days (Holl 2018), then at 42 days (6 weeks), approximately 67% will have been replaced by newly born neurons, and at 63 days (9 weeks), approximately 81% will have been replaced. At day 42, 3 weeks after the timepoint at which M71 counts were performed in initial experiments, we extracted the MOEs of male and female M71-GFP mice that underwent either unpaired or paired conditioning paradigms and optically cleared the tissue to compare M71 OSN abundance (Fig. 4C.). At the 42-day timepoint, we observed a 20% increase in the abundance of M71 OSNs in

paired animals compared to controls (Fig. 4C, S3A. Tukey's multiple comparisons. 42d unpaired vs. paired P=0.0476. n=8,8.). At 63 days, we observed a 30% increase in M71 OSNs in the paired group compared to controls (Fig. 4C, S3A. Tukey's multiple comparisons. 63d unpaired vs. paired P=0.0011. n=4,6.). The observation that these changes persist for at least 63 days after the start of conditioning, together with the reported 26-day half-life for the MOE, suggests the persistence of a signaling mechanism past the experience of olfactory fear conditioning itself.

To test whether a behavioral phenotype depends on OSN abundance, we performed an avoidance assay at the 42- and 63-day timepoints in a new cohort of mice. Mice were allowed 10 minutes to freely explore a 3-chamber arena (trichamber) in which the conditioned odor (acetophenone) was continuously delivered through a port on one side, and a control odor (propanol) on the other (Fig. 4D., Movie S1). We calculated an approach-avoid index as the difference in the amount of time spent on the conditioned odor side compared to the control odor side, normalized by the total time spent exploring either chamber (Fig. 4D.). A positive index indicates overall approach towards the conditioned odor, whereas a negative index indicates an aversion to the conditioned odor. At the 42-day timepoint, we observed no significant difference in the avoidance indices of unpaired and paired mice, with both groups exhibiting a slight aversion to acetophenone (Fig. 4E. Student's unpaired t-test. 42d unpaired vs. paired P=0.2248. n=10,11.). At the 63-day timepoint, we also observed no significant difference between the unpaired and paired mice (Fig. 4F. Student's unpaired t-test. 63d unpaired vs paired P=0.8987. n=6,8.). Interestingly, when accounting for sex, we found a significant aversion in female paired mice at the 42-day timepoint (Fig. S4A.) that was not present at the 63-day timepoint and not present at either timepoint in males (Fig. S4B-D). Despite the behavioral sex difference at day 42, we did not observe a significant sex difference in M71 OSN counts at the same timepoint (Fig. S3A.), indicating that the difference in behavior was not driven by a difference in MOE composition. Moreover, the absence of a strong behavioral aversion to acetophenone at 6- and 9-weeks post-conditioning despite a persistent increase in M71 representation in the MOE further suggests that an increase in OSN subtype following conditioning does not directly drive avoidance behavior. If this were the case, we would expect that the paired groups, which both exhibit heightened M71 counts at 42 and 63 days, would exhibit greater aversion to acetophenone than unpaired mice. Altogether, these results indicate that the mechanism underlying cellular adaptations in the MOE and the mechanism driving avoidance are independent.

Olfactory fear conditioning leads to nuanced behavioral differences in F1 offspring

To further disentangle the relationship between increased OSN subtype representation and avoidance behavior, we performed extensive analyses on both F0 and F1 behavior. We generated three parallel F0 and F1 cohorts with three odors: acetophenone, lyral, and propanol. In each cohort of mice in which F0 males were conditioned for F1 breeding, we also conditioned male and female mice and tested them in the trichamber assay the day after conditioning (Fig. 5B.). We used ANY-maze tracking software to track the center position of the mice for calculation of approach-avoid indices, as well as to measure metrics like speed, distance traveled, and freezing. Importantly, males that were used for F1 breeding were not tested in the trichamber prior to breeding to avoid extinction, which has been shown to reverse the increased OSN phenotype in both F0 and F1 (Aoued et al. 2019).

As expected, only mice in which odor and shock were paired exhibited robust aversion to the conditioned odor. F0 mice in the paired groups actively avoided the conditioned odor, whereas mice in the unpaired group exhibited no aversion to the conditioned odors (Fig. 5C, G, K. Tukey's multiple comparisons. F0 acetophenone unpaired vs. paired P<0.0001. n=10,15. F0 lyral unpaired vs. paired P<0.0001. n=17,20. F0 propanol unpaired vs. paired P<0.0001. n=16,20.). Naïve and unpaired mice spent roughly equal time exploring the control and conditioned odor chambers, whereas the paired mice spent an average of 67% (lyral-paired), 75% (acetophenone-paired), and 92% (propanol-paired) of the time exploring the control chamber.

Previous behavioral studies demonstrated that F1 offspring from fathers that experienced olfactory fear conditioning exhibit enhanced sensitivity to the conditioned odor in both odor potentiated startle and aversive odor association assays (Dias and Ressler 2014). Therefore, we asked whether we could detect aversive behavioral responses in F1 populations after conditioning F0 fathers. We decided to use the trichamber assay as opposed to assays used in previous studies because we were interested in whether offspring inherited, in addition to an increase in conditioned odor OSN representation, a behavioral aversion to the odor. F1 offspring generated from conditioned males and naïve females were assayed at 8- to 10-weeks of age in the same trichamber assay as the F0s. Importantly, none of the offspring had ever been exposed to the odor with which their father had been conditioned. We did not observe a significant difference in the avoidance indices of unpaired and paired F1 mice for any of the odors (Fig. 5C, G, K, S5, S6. Tukey's multiple comparisons. Acetophenone F1 unpaired vs. paired P=0.9999. n=22,18. Lyral F1 unpaired vs. paired P=0.9976. n=6,13. Propanol F1 unpaired vs. paired P=0.7935. n=13,13.).

Suspecting that our approach-avoid index may not be sensitive to more subtle behavioral differences, we performed additional behavioral analyses. Generation of spatial heat maps for the assays failed to reveal any clear qualitative differences in occupancy between unpaired and paired F1s in any of the three cohorts (Fig. 5D, H, L.). We also quantified freezing behavior during the trials and found no differences between unpaired and paired F1s in any of the cohorts (Fig. 5F, J, N.). However, we identified nuanced differences between unpaired and paired F1s that depended on the father's conditioned odor. When we quantified the distance traveled during the assay, we found that the F1s of lyral-paired fathers exhibited a hyperactive phenotype, traveling an average of 24.74 ± 0.74 meters during the 10-minute trial compared to 19.12 ± 1.66 meters in F1 lyral-unpaired mice (Fig. 5I, S5E. Tukey's multiple comparisons. Lyral F1 unpaired vs. paired P=0.0325. n=6,13.). Conversely, the F1s of propanol-paired fathers exhibited a hypoactive phenotype, traveling an average of 15.89 ± 1.11 meters compared to 23.33 ± 1.95 meters in F1 propanol-unpaired mice (Fig. 5M, S5H. Tukey's multiple comparisons. Propanol F1 unpaired vs. paired P=0.0045. n=13,13.). The phenotypes observed in the F1s of both lyral-paired and propanol-paired fathers are similarly reflected in the mean speeds of the mice during the trial, both of which were significantly different between the F1 unpaired and paired groups (Fig. S7D, G. Tukey's multiple comparisons. Lyral F1 unpaired vs. paired P=0.0315. n=6,13. Propanol F1 unpaired vs. paired P=0.0051. n=13,13.). We observed no significant differences in either distance traveled or mean speed in the F1s of acetophenone-conditioned fathers (Fig. 5E, S7A.). These analyses demonstrate that while the offspring of paired fathers do not actively

avoid their father's conditioned odor, odor-shock pairing leads to subtle behavioral differences in offspring, and that these differences are specific to the conditioned odor used.

Unsupervised machine learning analysis identifies behavioral differences in F1

To follow up on the differences observed between the F1s of unpaired and paired mice, we utilized Keypoint-MoSeq, a tool that uses unsupervised machine learning to identify behavioral modules, called "syllables," in an unbiased manner (Weinreb et al. 2024). First, we trained a SLEAP model to track eight keypoints (nose, right ear, left ear, neck, center, right leg, left leg, tail-base) on each mouse across the entire trial (Fig. 6B.) (Pereira et al. 2022). We trained a Keypoint-MoSeq model on the tracking data from 99 10-minute trichamber videos (30 F0 and 69 F1 videos), for a total of 1.78×10^6 frames, to identify behavioral syllables with a median duration of approximately 30 frames (1 second) (Fig. 6B, C.). This allowed us to ask whether the differences we observed between lyral F1s and propanol F1s at the timescale of 10 minutes could be tied to specific behaviors at the timescale of seconds, rather than a summary of 10 minutes. In our first analysis, we grouped the F1s of acetophenone-, lyral-, and propanol-unpaired fathers, and grouped the F1s of acetophenone-, lyral-, and propanol-paired fathers, to investigate whether there are differences between unpaired and paired offspring that generalize across the conditioned odors. Strikingly, we identified four syllables (3, 5, 11, and 22) with a significant difference in relative frequency (usage) between unpaired and paired F1s (Fig. 6D. Kruskal-Wallis test with Dunn's multiple comparisons. F1 unpaired vs. paired. Syllable 3 P=0.0070. Syllable 5 P=0.0054. Syllable 11 P=0.0251. Syllable 22 P=0.0184.). Of those four syllables, syllables 3 and 5 were used significantly more in the F1 paired group compared to the F1 unpaired group, while syllables 11 and 22 were used significantly less in the F1 paired group (Fig. 6D.). We also noticed interesting qualitative differences in the spatial usage patterns of each syllable, with unpaired and paired F1s showing distinct usage distributions relative to their distance from the conditioned odor port (Fig. S8.). Next, we were interested in behavioral differences specifically in response to the conditioned odor of the parent. To this end, we narrowed the analysis to syllable usage only when the mouse was in the conditioned odor chamber. While both F1 unpaired and F1 paired mice spent similar amounts of time in the conditioned odor chamber (Fig. 6E., Fig. S7C, F, I.), the F1 paired group exhibited greater usage of syllables 5 and 17 compared to controls (Fig. 6F. Kruskal-Wallis test with Dunn's multiple comparisons. F1 unpaired vs. paired. Syllable 5 P=0.0406. Syllable 17 P=0.0467). Taken together, these findings point to small but significant behavioral differences between the offspring of unpaired and paired fathers that generalize across all three conditioning odors.

Lastly, we performed the same analysis separately for the three F1 cohorts of acetophenone-, lyral-, and propanol-conditioned F0 fathers. Interestingly, in parallel with the earlier analyses, we again observed no differences between the unpaired and paired F1s of acetophenone-conditioned fathers (Fig. 6G.) despite differences in M71 OSN representation. Also consistent with our earlier analyses, we found significant differences between the unpaired and paired F1s of lyral- and propanol-conditioned fathers, and the differences between the unpaired and paired F1 groups were unique to the odor (Fig. 6H, I.). We identified six syllables with significantly different frequencies between unpaired and paired F1s of lyral-conditioned fathers: 2, 3, 5, 7, 15, and 20 (Fig. 6H. Kruskal-Wallis test with Dunn's multiple comparisons. Lyral F1 unpaired vs. paired. Syllable 2 P=0.0016. Syllable 3 P=0.0272. Syllable 5 P=0.0030. Syllable 7 P=0.0025. Syllable 15 P=0.0208. Syllable 20 P=0.0002.). The upregulated syllables in

lyral paired F1s were higher-velocity syllables, while the downregulated syllables were relatively stationary/low-velocity, consistent with the hyperactive phenotype earlier described by greater distance traveled and higher mean speed in lyral-paired F1s. Between the unpaired and paired F1s of propanol-conditioned fathers, we found five syllables with significantly different frequencies: 6, 12, 14, 15, and 20 (Fig. 6I. Kruskal-Wallis test with Dunn's multiple comparisons. Propanol F1 unpaired vs. paired. Syllable 6 P=0.0206. Syllable 12 P=0.0407. Syllable 14 P=0.0072. Syllable 15 P=0.0320. Syllable 20 P=0.0148.). Compared to the lyral F1s, the opposite was true for the differentially used syllables in the propanol F1s, in which the upregulated syllables in propanol-paired F1s were lower-velocity syllables, and the downregulated syllables were relatively high-velocity syllables, consistent with the hypoactive phenotype earlier described. Here, we have demonstrated that olfactory fear conditioning in the F0 population leads to conditioned odor-specific effects in the F1 offspring of paired mice.

Discussion

We used tissue-clearing and light-sheet microscopy to demonstrate a specific increase in the number of OSNs expressing the receptor for an aversively conditioned odor. Enhanced abundance of OSNs responsive to the conditioned odor were observed in naïve F1 offspring of conditioned F0 males. These results are consistent with studies that employ other cellular visualization techniques (Dias and Ressler 2014; Aoued et al. 2019; 2020). In F0, this increase is stable for at least 63 days, a time by which most of the cells present during olfactory fear conditioning have been replaced by newborn sensory neurons. The increase in OSN count in F0 results, in part, from the contribution of newborn neurons responsive to the conditioned odor, demonstrating a biasing of OSN development. The sustained increase in F0, along with the inheritance in F1, suggests that there is a stable signal that is responsible for the induction, maintenance, and inheritance of the increase in OSNs responsive to the paired odor.

The stochastic choice of olfactory receptors may provide an opportunity to alter the representation of receptors to allow an organism to adapt to the environment. Changes in the number of OSNs may lead to an increase in sensitivity of the paired odor. A change in OSN number may also lead to increased inputs to downstream sensory areas. Such perceptual changes have been reported in the motor, visual, olfactory, and auditory systems, where topographical arrangements at the primary sensory cortex are modulated in certain fear conditioning paradigms in mammals (Ressler et al. 1994; Vassar et al. 1994, 199; Mombaerts et al. 1996; Lai et al. 2018; Xu et al. 2019; Li et al. 2019), although this has not yet been demonstrated intergenerationally. We observed an increase in conditioned odor-responsive neurons in both the F0 and F1 populations. Only the F0, however, exhibited active avoidance behavior. Interestingly, the F0 paired groups exhibited varying degrees of avoidance based on the odor used in conditioning (Fig. 5.). Similarly, the effects that we observed in the F1 offspring of paired mice depended on the conditioning odor of the father. This presents the possibility that factors such as odor volatility, the abundance of odor-responsive OSN populations, and the binding affinities of those populations, may influence the behavioral phenotypes in both parent and offspring despite the shared cellular phenotype of increased OSN abundance. We speculate that the increase in neurons responsive to the conditioned odor could enhance the sensitivity to, or the discrimination of, the paired odor in F0 and F1. This would enable the F1 population to learn that odor predicts shock with fewer training cycles or less odor when trained with the conditioned odor.

These findings set a foundation to uncover the mechanism by which olfactory receptor bias is communicated within the main olfactory epithelium, to the germline, and, moreover, maintained during the development of offspring. What remains to be uncovered are the mechanisms to bias the choice of specific receptors in the main olfactory epithelium and how the information governing the biasing of receptor choice is transferred to the gametes. In mice, the paternal transmission of epigenetic information has been observed following metabolic disturbances, social stress, and exposure to drugs and toxins (Huypens et al. 2016). High-fat or low-protein diets, as well as caloric restriction in the father, results in metabolic disturbances in the offspring, even after *in vitro* fertilization (Carone et al. 2010; Q. Chen et al. 2016). Parental stressors, such as chronic defeat or maternal separation, result in hormonal disturbances and behavioral phenotypes in the offspring (Dietz et al. 2011; Morgan and Bale 2011; Gapp et al. 2014). Finally, toxins and addictive drugs result in an array of metabolic disturbances in the F1 population that recapitulate the paternal state (Toussaint et al. 2022). These paternal stressors are associated with metabolic and hormonal disturbances that can readily act at a distance to affect the gamete. It has been demonstrated in male gametogenesis that extracellular vesicles in the testes transmit an RNA payload as they fuse with maturing sperm (Rando 2016; Sharma et al. 2018; Morgan et al. 2019; Chan et al. 2020). Such studies provide insights into a mechanism by which an olfactory sensory experience paired with fear learning could transmit receptor-specific information from one generation to the next.

Controversies surrounding heritable behaviors in mammals hinge on the question of what biological adaptations can be inherited that would lead to alterations in the behavior of future generations. We focused on the ethological behavior of olfactory avoidance and observed nuanced behaviors in the F1 population that have not formerly been described. We hypothesize that these changes in behavior are related to the inheritance of an increase in specific OSN populations, but the question remains whether there are heritable changes in downstream brain circuits that could contribute to a behavioral phenotype. Multiple results lead us to believe that changes in OSN representation in the MOE are not sufficient to drive olfactory avoidance of the conditioned odor. First, we observe robust avoidance of the conditioned odor one day after olfactory fear conditioning, at which point we expect minimal effects of biased neurogenesis given the rates of OSN maturation and turnover in the MOE. Thus, the behavioral effects in F0 likely do not require an increase in conditioned odor-responsive OSN abundance. Second, we observe the persistence of an increase in M71 OSN representation at the 42- and 63-day timepoints, when mice no longer avoid the conditioned odor, indicating that higher cell number alone does not drive avoidance. Lastly, the F1 offspring of paired males do not actively avoid the conditioned odor despite exhibiting higher numbers of conditioned odor-responsive OSNs. This disentanglement of cell number and avoidance behavior leads to the hypothesis that, in parallel with the inheritance of the MOE phenotype, changes to brain circuits responding to stress may also be inherited. One possibility is that heritable changes in neuromodulator systems could shift the balance of internal states in offspring, as has been observed in rodent studies (Champagne 2008; Rodgers et al. 2013; Gapp et al. 2021).

Our study elaborates on a function of sensory systems in which a learned adaptation can influence future generations. Thus, the distinction between innate and learned behaviors may be fundamentally flexible — learned adaptations in the parent may have the potential to become

innate in their offspring. Understanding the mechanisms of inherited adaptation will provide insight for interventions when these changes no longer serve as adaptive to the organism.

References and Notes

Aoued, Hadj S., Soma Sannigrahi, Nandini Doshi, et al. 2019. "Reversing Behavioral, Neuroanatomical, and Germline Influences of Intergenerational Stress." *Biological Psychiatry* 85 (3): 248–56. https://doi.org/10.1016/j.biopsych.2018.07.028.

Aoued, Hadj S., Soma Sannigrahi, Sarah C. Hunter, et al. 2020. "Proximate Causes and Consequences of Intergenerational Influences of Salient Sensory Experience." *Genes, Brain and Behavior* 19 (4): e12638. https://doi.org/10.1111/gbb.12638.

Bozza, Thomas, Paul Feinstein, Chen Zheng, and Peter Mombaerts. 2002. "Odorant Receptor Expression Defines Functional Units in the Mouse Olfactory System." ARTICLE. *Journal of Neuroscience* 22 (8): 3033–43. https://doi.org/10.1523/JNEUROSCI.22-08-03033.2002.

Buck, L., and R. Axel. 1991. "A Novel Multigene Family May Encode Odorant Receptors: A Molecular Basis for Odor Recognition." *Cell* 65 (1): 175–87. https://doi.org/10.1016/0092-8674(91)90418-x.

Cadiou, Hervé, Imad Aoudé, Bassim Tazir, et al. 2014. "Postnatal Odorant Exposure Induces Peripheral Olfactory Plasticity at the Cellular Level." *The Journal of Neuroscience: The Official Journal of the Society for Neuroscience* 34 (14): 4857–70. https://doi.org/10.1523/JNEUROSCI.0688-13.2014.

Carone, Benjamin R., Lucas Fauquier, Naomi Habib, et al. 2010. "Paternally Induced Transgenerational Environmental Reprogramming of Metabolic Gene Expression in Mammals." *Cell* 143 (7): 1084–96. https://doi.org/10.1016/j.cell.2010.12.008.

Champagne, Frances A. 2008. "Epigenetic Mechanisms and the Transgenerational Effects of Maternal Care." *Frontiers in Neuroendocrinology*, Special Issue: Epigenetics, vol. 29 (3): 386–97. https://doi.org/10.1016/j.yfrne.2008.03.003.

Chan, Jennifer C., Christopher P. Morgan, N. Adrian Leu, et al. 2020. "Reproductive Tract Extracellular Vesicles Are Sufficient to Transmit Intergenerational Stress and Program Neurodevelopment." *Nature Communications* 11 (1): 1. https://doi.org/10.1038/s41467-020-15305-w.

Chen, Chien-Fu F., Dong-Jing Zou, Clara G. Altomare, Lu Xu, Charles A. Greer, and Stuart J. Firestein. 2014. "Nonsensory Target-Dependent Organization of Piriform Cortex." *Proceedings of the National Academy of Sciences* 111 (47): 16931–36. https://doi.org/10.1073/pnas.1411266111.

Chen, Qi, Menghong Yan, Zhonghong Cao, et al. 2016. "Sperm tsRNAs Contribute to Intergenerational Inheritance of an Acquired Metabolic Disorder." *Science* 351 (6271): 397–400. https://doi.org/10.1126/science.aad7977.

Cheraghali, A. M., R. Kumar, E. E. Knaus, and L. I. Wiebe. 1995. "Pharmacokinetics and Bioavailability of 5-Ethyl-2'-Deoxyuridine and Its Novel (5R,6R)-5-Bromo-6-Ethoxy-5,6-Dihydro Prodrugs in Mice." *Drug Metabolism and Disposition* 23 (2): 223–26.

Chess, Andrew, Itamar Simon, Howard Cedar, and Richard Axel. 1994. "Allelic Inactivation Regulates Olfactory Receptor Gene Expression." *Cell* 78 (5): 823–34. https://doi.org/10.1016/S0092-8674(94)90562-2.

Cunningham, Ashley M., Deena M. Walker, Aarthi Ramakrishnan, et al. 2021. "Sperm Transcriptional State Associated with Paternal Transmission of Stress Phenotypes." Research Articles. *Journal of Neuroscience* 41 (29): 6202–16. https://doi.org/10.1523/JNEUROSCI.3192-20.2021.

Dias, Brian G, and Kerry J Ressler. 2014. "Parental Olfactory Experience Influences Behavior and Neural Structure in Subsequent Generations." *Nature Neuroscience* 17 (1): 89–96. https://doi.org/10.1038/nn.3594.

Dietz, David M., Quincey Laplant, Emily L. Watts, et al. 2011. "Paternal Transmission of Stress-Induced Pathologies." *Biological Psychiatry* 70 (5): 408–14. https://doi.org/10.1016/j.biopsych.2011.05.005.

Diodato, A., M. Ruinart De Brimont, Y.S. Yim, et al. 2016. "Molecular Signatures of Neural Connectivity in the Olfactory Cortex." *Nature Communications* 7. Scopus. https://doi.org/10.1038/ncomms12238.

Fitz-James, Maximilian H., and Giacomo Cavalli. 2022. "Molecular Mechanisms of Transgenerational Epigenetic Inheritance." *Nature Reviews Genetics*, January 4, 1–17. https://doi.org/10.1038/s41576-021-00438-5.

Gapp, Katharina, Ali Jawaid, Peter Sarkies, et al. 2014. "Implication of Sperm RNAs in Transgenerational Inheritance of the Effects of Early Trauma in Mice." *Nature Neuroscience* 17 (5): 667–69. https://doi.org/10.1038/nn.3695.

Gapp, Katharina, Guillermo E. Parada, Fridolin Gross, et al. 2021. "Single Paternal Dexamethasone Challenge Programs Offspring Metabolism and Reveals Multiple Candidates in RNA-Mediated Inheritance." *iScience* 24 (8): 102870. https://doi.org/10.1016/j.isci.2021.102870.

Greer, Eric L., Travis J. Maures, Duygu Ucar, et al. 2011. "Transgenerational Epigenetic Inheritance of Longevity in Caenorhabditis Elegans." *Nature* 479 (7373): 7373. https://doi.org/10.1038/nature10572.

Holl, Anna-Maria. 2018. "Survival of Mature Mouse Olfactory Sensory Neurons Labeled Genetically Perinatally." *Molecular and Cellular Neurosciences* 88 (April): 258–69. https://doi.org/10.1016/j.mcn.2018.02.005.

Huypens, Peter, Steffen Sass, Moya Wu, et al. 2016. "Epigenetic Germline Inheritance of Diet-Induced Obesity and Insulin Resistance." *Nature Genetics* 48 (5): 497–99. https://doi.org/10.1038/ng.3527.

Johnson, Brett A., and Michael Leon. 2000. "Modular Representations of Odorants in the Glomerular Layer of the Rat Olfactory Bulb and the Effects of Stimulus Concentration." *Journal of Comparative Neurology* 422 (4): 496–509. https://doi.org/10.1002/1096-9861(20000710)422:4<496::AID-CNE2>3.0.CO;2-4.

Jones, Seth V., Dennis C. Choi, Michael Davis, and Kerry J. Ressler. 2008. "Learning-Dependent Structural Plasticity in the Adult Olfactory Pathway." *The Journal of Neuroscience* 28 (49): 13106–11. https://doi.org/10.1523/JNEUROSCI.4465-08.2008.

Lai, Cora Sau Wan, Avital Adler, and Wen-Biao Gan. 2018. "Fear Extinction Reverses Dendritic Spine Formation Induced by Fear Conditioning in the Mouse Auditory Cortex." *Proceedings of the National Academy of Sciences* 115 (37): 9306–11. https://doi.org/10.1073/pnas.1801504115.

Li, Zhihan, An Yan, Kun Guo, and Wu Li. 2019. "Fear-Related Signals in the Primary Visual Cortex." *Current Biology* 29 (23): 4078-4083.e2. https://doi.org/10.1016/j.cub.2019.09.063.

Liberia, Teresa, Eduardo Martin-Lopez, Sarah J. Meller, and Charles A. Greer. 2019. "Sequential Maturation of Olfactory Sensory Neurons in the Mature Olfactory Epithelium." *Eneuro* 6 (5): ENEURO.0266-19.2019. https://doi.org/10.1523/ENEURO.0266-19.2019.

Lomvardas, Stavros, Gilad Barnea, David J. Pisapia, Monica Mendelsohn, Jennifer Kirkland, and Richard Axel. 2006. "Interchromosomal Interactions and Olfactory Receptor Choice." *Cell* 126 (2): 403–13. https://doi.org/10.1016/j.cell.2006.06.035.

Mombaerts, Peter, Fan Wang, Catherine Dulac, et al. 1996. "Visualizing an Olfactory Sensory Map." *Cell* 87 (4): 675–86. https://doi.org/10.1016/S0092-8674(00)81387-2.

Moore, Rebecca S., Rachel Kaletsky, Chen Lesnik, et al. 2021. "The Role of the Cer1 Transposon in Horizontal Transfer of Transgenerational Memory." *Cell* 184 (18): 4697-4712.e18. https://doi.org/10.1016/j.cell.2021.07.022.

Morgan, Christopher P., and Tracy L. Bale. 2011. "Early Prenatal Stress Epigenetically Programs Dysmasculinization in Second-Generation Offspring via the Paternal Lineage." Articles. *Journal of Neuroscience* 31 (33): 11748–55. https://doi.org/10.1523/JNEUROSCI.1887-11.2011.

Morgan, Christopher P., Jennifer Chan, and Tracy L. Bale. 2019. "Driving the next Generation: Paternal Lifetime Experiences Transmitted via Extracellular Vesicles and Their Small RNA Cargo." *Biological Psychiatry* 85 (2): 164–71. https://doi.org/10.1016/j.biopsych.2018.09.007.

Pereira, Talmo D., Nathaniel Tabris, Arie Matsliah, et al. 2022. "SLEAP: A Deep Learning System for Multi-Animal Pose Tracking." *Nature Methods* 19 (4): 486–95. https://doi.org/10.1038/s41592-022-01426-1.

Price, J. L., and T. P. S. Powell. 1970. "The Mitral and Short Axon Cells of the Olfactory Bulb." *Journal of Cell Science* 7 (3): 631–51. https://doi.org/10.1242/jcs.7.3.631.

Price, Joseph L. 1985. "Beyond the Primary Olfactory Cortex: Olfactory-Related Areas in the Neocortex, Thalamus and Hypothalamus." *Chemical Senses* 10 (2): 239–58. https://doi.org/10.1093/chemse/10.2.239.

Rando, Oliver J. 2016. "Intergenerational Transfer of Epigenetic Information in Sperm." *Cold Spring Harbor Perspectives in Medicine* 6 (5): a022988. https://doi.org/10.1101/cshperspect.a022988.

Rando, Oliver J., and Kevin J. Verstrepen. 2007. "Timescales of Genetic and Epigenetic Inheritance." *Cell* 128 (4): 655–68. https://doi.org/10.1016/j.cell.2007.01.023.

Rechavi, Oded, Leah Houri-Ze'evi, Sarit Anava, et al. 2014. "Starvation-Induced Transgenerational Inheritance of Small RNAs in C. Elegans." *Cell* 158 (2): 277–87. https://doi.org/10.1016/j.cell.2014.06.020.

Renier, Nicolas, Eliza L. Adams, Christoph Kirst, et al. 2016. "Mapping of Brain Activity by Automated Volume Analysis of Immediate Early Genes." *Cell* 165 (7): 1789–802. https://doi.org/10.1016/j.cell.2016.05.007.

Ressler, Kerry J., Susan L. Sullivan, and Linda B. Buck. 1994. "Information Coding in the Olfactory System: Evidence for a Stereotyped and Highly Organized Epitope Map in the Olfactory Bulb." *Cell* 79 (7): 1245–55. https://doi.org/10.1016/0092-8674(94)90015-9.

Rodgers, Ali B., Christopher P. Morgan, Stefanie L. Bronson, Sonia Revello, and Tracy L. Bale. 2013. "Paternal Stress Exposure Alters Sperm MicroRNA Content and Reprograms Offspring HPA Stress Axis Regulation." Articles. *Journal of Neuroscience* 33 (21): 9003–12. https://doi.org/10.1523/JNEUROSCI.0914-13.2013.

590 Schmitz, Robert J., Matthew D. Schultz, Mathew G. Lewsey, et al. 2011. "Transgenerational Epigenetic Instability Is a Source of Novel Methylation Variants." *Science* 334 (6054): 369–73. https://doi.org/10.1126/science.1212959.

Sharma, Upasna, Fengyun Sun, Colin C. Conine, et al. 2018. "Small RNAs Are Trafficked from the Epididymis to Developing Mammalian Sperm." *Developmental Cell* 46 (4): 481-
595 494.e6. https://doi.org/10.1016/j.devcel.2018.06.023.

Shykind, Benjamin M., S. Christy Rohani, Sean O'Donnell, et al. 2004. "Gene Switching and the Stability of Odorant Receptor Gene Choice." *Cell* 117 (6): 801–15. https://doi.org/10.1016/j.cell.2004.05.015.

Touhara, K., S. Sengoku, K. Inaki, et al. 1999a. "Functional Identification and Reconstitution of
600 an Odorant Receptor in Single Olfactory Neurons." *Proceedings of the National Academy of Sciences of the United States of America* 96 (7): 4040–45. https://doi.org/10.1073/pnas.96.7.4040.

Touhara, Kazushige, Shintaro Sengoku, Koichiro Inaki, et al. 1999b. "Functional Identification and Reconstitution of an Odorant Receptor in Single Olfactory Neurons." *Proceedings of*
605 *the National Academy of Sciences* 96 (7): 4040–45. https://doi.org/10.1073/pnas.96.7.4040.

Toussaint, Andre B., William Foster, Jessica M. Jones, et al. 2022. "Chronic Paternal Morphine Exposure Increases Sensitivity to Morphine-Derived Pain Relief in Male Progeny." *Science Advances* 8 (7): eabk2425. https://doi.org/10.1126/sciadv.abk2425.

610 Vassar, Robert, Steve K. Chao, Raquel Sitcheran, Jennifer M. Nun˜ez, Leslie B. Vosshall, and Richard Axel. 1994. "Topographic Organization of Sensory Projections to the Olfactory Bulb." *Cell* 79 (6): 981–91. https://doi.org/10.1016/0092-8674(94)90029-9.

Weinreb, Caleb, Jonah E. Pearl, Sherry Lin, et al. 2024. "Keypoint-MoSeq: Parsing Behavior by Linking Point Tracking to Pose Dynamics." *Nature Methods* 21 (7): 1329–39.
615 https://doi.org/10.1038/s41592-024-02318-2.

Xu, Zhiwei, Avital Adler, Hong Li, et al. 2019. "Fear Conditioning and Extinction Induce Opposing Changes in Dendritic Spine Remodeling and Somatic Activity of Layer 5 Pyramidal Neurons in the Mouse Motor Cortex." *Scientific Reports* 9 (1): 1. https://doi.org/10.1038/s41598-019-40549-y.

620 Yu, Ruby, Xiaoyi Wang, and Danesh Moazed. 2018. "Epigenetic Inheritance Mediated by Coupling of RNAi and Histone H3K9 Methylation." *Nature* 558 (7711): 615–19. https://doi.org/10.1038/s41586-018-0239-3.

625 **Acknowledgements:** We thank the past and current members of the Marlin Lab for critical discussions and inputs on the manuscript. We thank Dr. D. Ng and Zuckerman Institute's Genetic Access Tools platform for generating the M71-IRES-tauRFP2 mouse line. We thank Drs. R. Axel, S. Lomvardas, C. Mason, I. Abdus-Saboor, I. Ahmed, and J. J. Marlin for their comments and discussion. We thank A.I.S.C, A.M., and V.L.F.N. for their support. Imaging was performed
630 with support from the Zuckerman Institute's Cellular Imaging platform.

Funding:

Simons Society of Fellows Junior Fellowship 524991 (BJM)

UNCF E.E. Just Fellowship CU20-1071 (BJM)

BBRF NARSAD Young Investigator Grant 30380 (BJM)
Howard Hughes Medical Institute (BJM)
National Institutes of Mental Health grant T32MH126036 (CWL)
National Institutes of Health grant 1S10OD023587-01 (Z.I. Cellular Imaging)

Author contributions:

Conceptualization: CWL, YRA, BJM
Methodology: CWL, YRA, ECBJ, HSL, BJM
Investigation: CWL, YRA, ECBJ, HSL, AC, AK, DKDF, AVA, BJM
Visualization: CWL, BJM
Funding acquisition: BJM
Project administration: CWL, BJM
Supervision: BJM
Writing – original draft: CWL, YRA, BJM
Writing – review & editing: CWL, BJM

Competing interests: Authors declare that they have no competing interests.

Data and materials availability: All data are available upon request.

Supplementary Materials

Materials and Methods
Supplementary Figs. S1 to S8
Movies S1 to S7
Tables S1 to S2

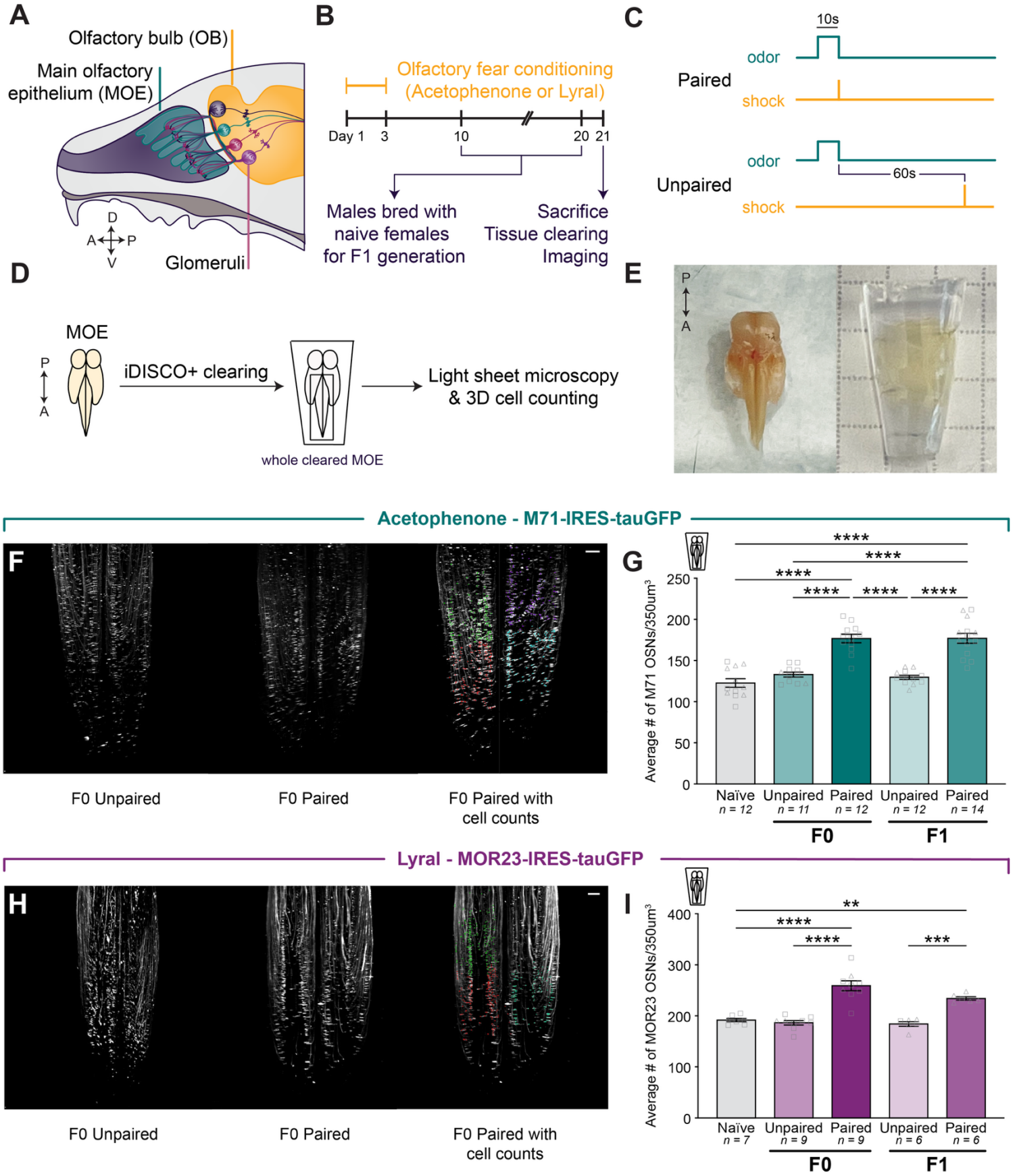

Fig. 1. Olfactory fear conditioning leads to an increase in conditioned-odor-responsive cells in parents (F0) that is heritable (F1). (A) Schematic representation of the mouse main olfactory

epithelium and olfactory bulb. MOE: main olfactory epithelium. OB: olfactory bulb. **(B)** Timeline of olfactory fear conditioning, breeding for the F1 generation, and MOE collection. **(C)** Experimental paradigms for olfactory fear conditioning groups. Mice in the paired condition received a foot shock that co-terminated with odor presentation, while mice in the unpaired condition received a foot shock 60 seconds after odor presentation. **(D)** Schematic demonstrating the process by which cells of interest in the MOE were quantified. Epithelia from both M71-IRES-tauGFP$^{+/+}$ and MOR23-IRES-tauGFP$^{+/+}$ adult mice were cleared using the iDISCO+ tissue-clearing protocol. Samples were imaged on a light sheet microscope and analyzed using Imaris spot detection software. **(E)** Images of the MOE before (left) and after (right) optical tissue clearing. **(F)** Example images of M71 OSNs in zone 1 of cleared MOE from both the unpaired (left) and paired (middle) conditions. Example image of an MOE with the counted cells represented by colored dots (right). Each set of colors represents a distinct counting cube. Scale bar: 200µm. **(G)** The average number of M71 OSNs in a 350^3 μm^3 cube of epithelium of naïve (gray), acetophenone unpaired (lighter green), and acetophenone paired (darker green) conditions in F0 and F1 (One-way ANOVA. P<0.0001. Tukey's multiple comparisons. Naïve vs. F0 paired P<0.0001. F0 unpaired vs. paired P<0.0001. Naïve vs. F1 paired P<0.0001. F1 unpaired vs. paired P<0.0001. n=12,11,12,12,14.). Squares indicate males, triangles indicate females. **(H)** Example images of MOR23 OSNs in zone 1 of cleared MOE from both the unpaired (left) and paired (middle) conditions. Example image of an MOE with the counted cells represented by colored dots (right). Scale bar: 200µm. **(I)** The average number of MOR23 OSNs in a 350^3 μm^3 cube of epithelium in naïve (gray), lyral unpaired (lighter purple), and lyral paired (darker purple) conditions in F0 and F1 (One-way ANOVA. P<0.0001. Tukey's multiple comparisons. Naïve vs. F0 paired P=<0.0001. F0 unpaired vs. paired P<0.0001. F1 unpaired vs. paired P=0.0368. n=7,9,9,6,6.).

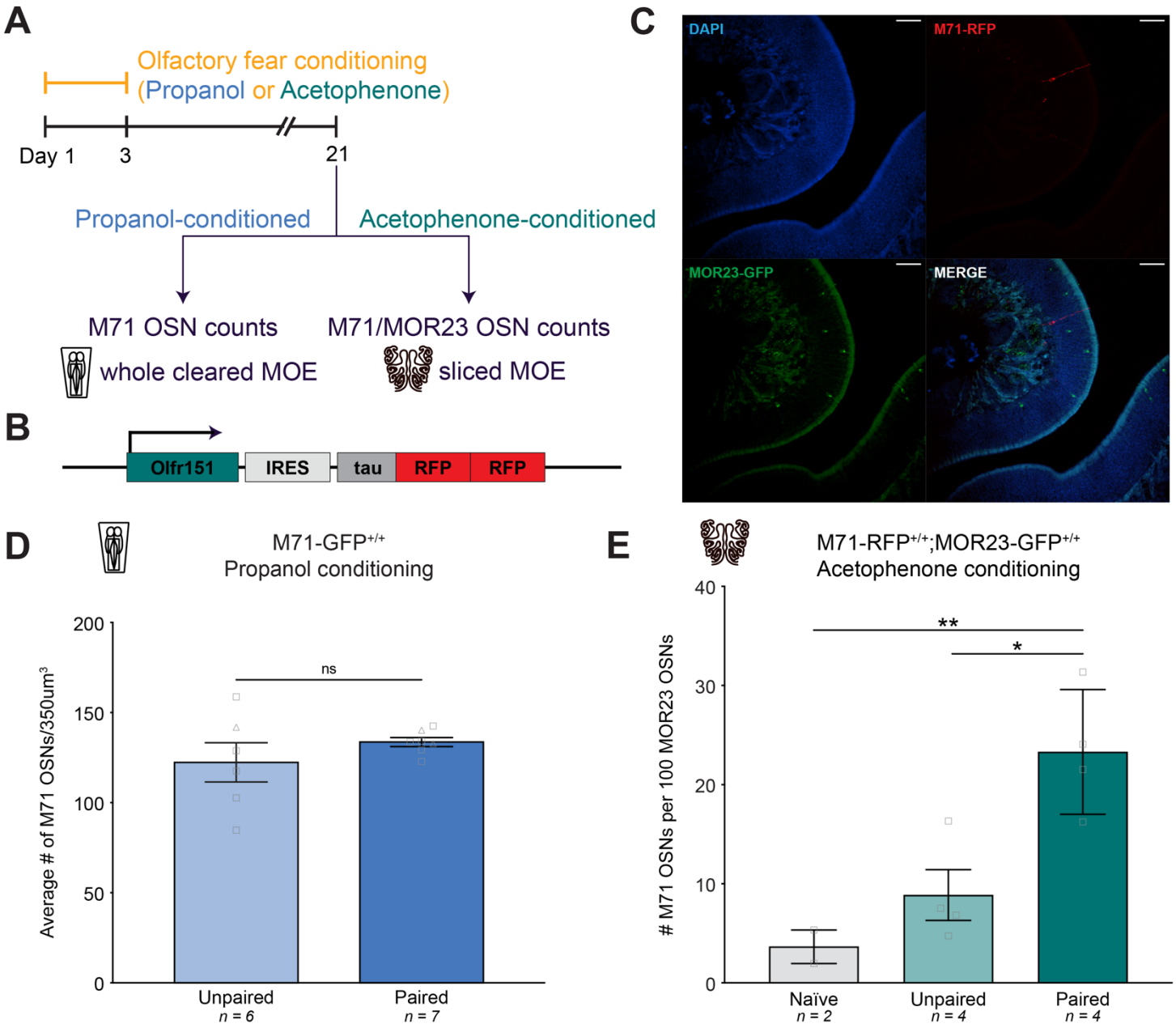

Fig. 2. Increased OSN abundance is specific to OSN subtypes responsive to the conditioned odor. (A) Timeline of olfactory fear conditioning and MOE collection for both experiments. **(B)** M71-IRES-tauRFP$_2$ targeted mutation. **(C)** Representative images showing DAPI (blue, top left), endogenous RFP in M71 OSNs (red, top right), endogenous GFP in MOR23 OSNs (green, bottom left), and the merged channels (bottom right) in an M71-RFP$^{+/+}$;MOR23GFP$^{+/+}$ animal. Scale bar: 50µm. **(D)** The average number of M71 olfactory sensory neurons in a 350^3 µm^3 cube of the epithelium in the propanol unpaired (light blue) and propanol paired (dark blue) conditions (Student's unpaired t-test. Unpaired vs. paired P=0.3009. n=6,7.). Squares indicate males, triangles indicate females. **(E)** The ratio of M71 OSNs to 100 MOR23 OSNs in M71-RFP$^{+/+}$;MOR23GFP$^{+/+}$ mice following no conditioning (naïve, gray), unpaired (light green), or paired (dark green) olfactory fear conditioning with acetophenone (One-way ANOVA. P=0.0062. Tukey's multiple comparisons. Naïve vs. paired P=0.0097. Unpaired vs. paired P=0.0163. n=2,4,4.).

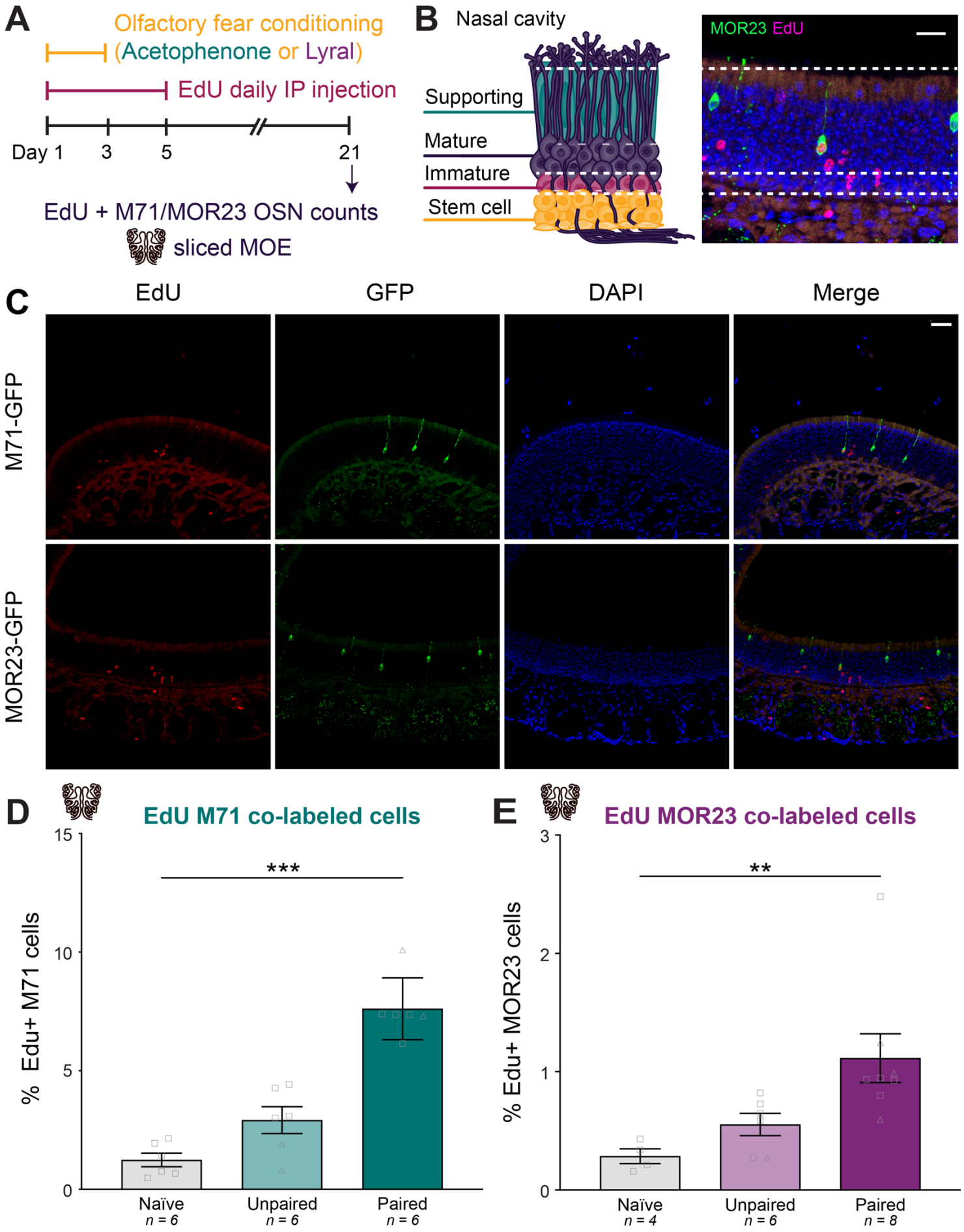
A
Olfactory fear conditioning
(Acetophenone or Lyral)
EdU daily IP injection
Day 1
3
5
21
EdU + M71/MOR23 OSN counts
sliced MOE
B
Nasal cavity
Supporting
Mature
Immature
Stem cell
MOR23 EdU
C
EdU
GFP
DAPI
Merge
M71-GFP
MOR23-GFP
D
EdU M71 co-labeled cells
% Edu+ M71 cells
***
Naïve
n = 6
Unpaired
n = 6
Paired
n = 6
E
EdU MOR23 co-labeled cells
% Edu+ MOR23 cells
**
Naïve
n = 4
Unpaired
n = 6
Paired
n = 8

Fig. 3. Olfactory fear conditioning biases olfactory receptor choice toward conditioned-odor-responsive cell-specific identities. (A) Timeline of olfactory fear conditioning, EdU injections, and MOE collection. **(B)** Schematic representation of the layers of the MOE, showing the stem cell, immature OSN, and mature OSN populations (left). Representative image of the MOE from an MOR23GFP$^{+/+}$ mouse showing EdU-positive cells (magenta) and a newborn (EdU+) MOR23 OSN (green and magenta). Scale bar: 20 µm. **(C)** Representative images showing MOE staining of EdU (red, first column), endogenous GFP (green, second column), DAPI (blue, third column), and the merged channels (fourth column) in both M71GFP$^{+/+}$ and MOR23GFP$^{+/+}$ mice. Scale bar: 40µm. **(D)** Percentage of EdU-positive M71 OSNs in naïve, unpaired, and paired groups (Kruskal-Wallis test. P<0.0001. Dunn's multiple comparisons. Naïve vs. paired P=0.0009. Unpaired vs. paired P=0.0799. n=6,6,6.). Squares indicate males, triangles indicate females. **(E)** Percentage of EdU-positive MOR23 OSNs in naïve, unpaired, and paired groups (Kruskal-Wallis test. P=0.0003. Dunn's multiple comparisons. Naïve vs. paired P=0.0040. Unpaired vs. paired P=0.0725. n=4,6,8.).

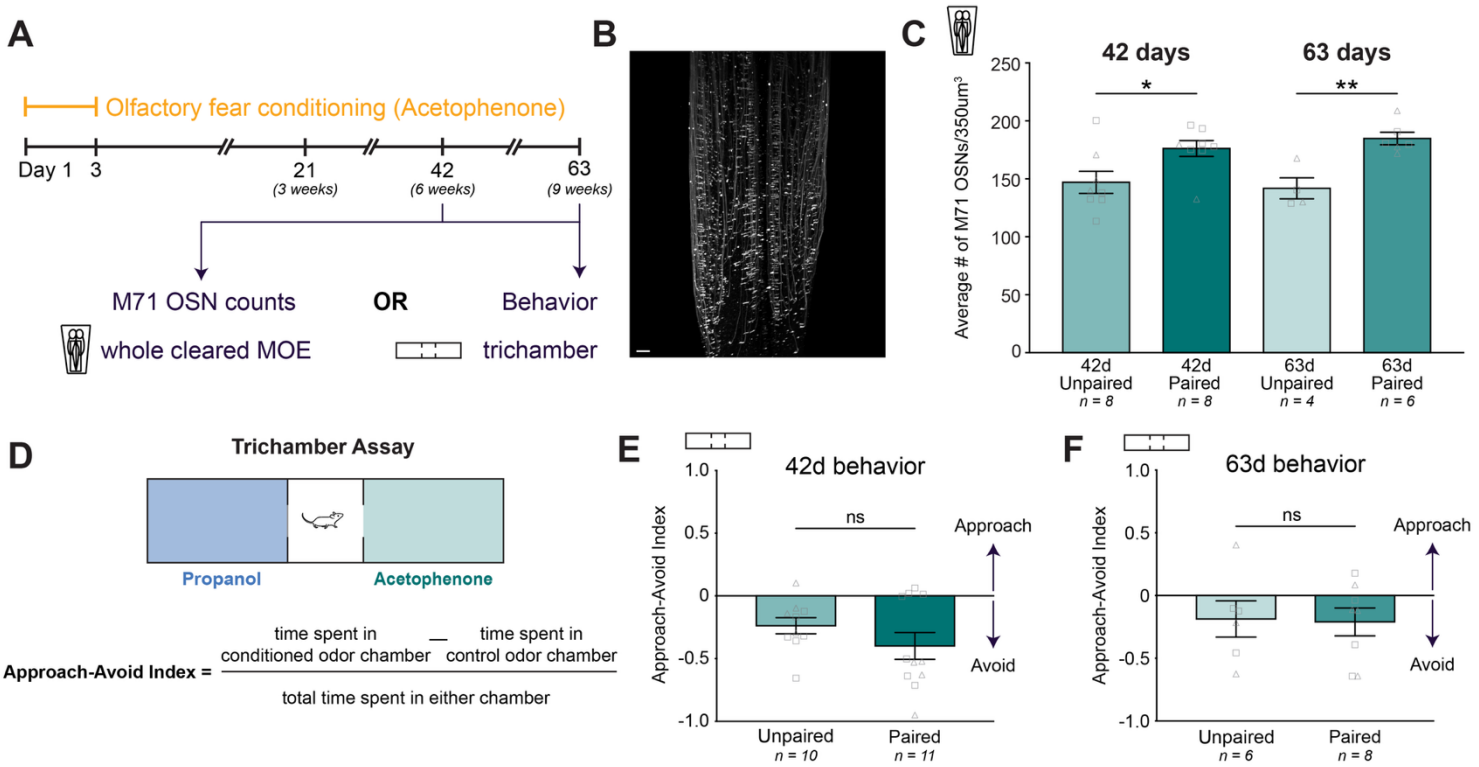

Fig. 4. Conditioned-odor-responsive cell increase is sustained through at least 9 weeks of cell turnover. **(A)** Timeline of olfactory fear conditioning and extended MOE collection time points. (B) Example image of M71 OSNs in zone 1 of cleared MOE collected 42 days post-conditioning. Scale bar: 200µm. **(C)** The average number of M71 OSNs in a 350^3 μm^3 cube of epithelium of unpaired (light green) and paired (dark green) mice, 42- or 63-days post-conditioning (One-way ANOVA. P=0.0033. Tukey's multiple comparisons. 42d unpaired vs. paired P=0.0476. 63d unpaired vs. paired P=0.0203. n=8,8,4,6.). Squares indicate males, triangles indicate females. **(D)** Schematic of the trichamber behavioral approach-avoidance assay and equation for the approach-avoid index. Positive values indicate approach to the conditioned odor (acetophenone), while negative values indicate avoidance. **(E)** The approach-avoid indices of unpaired and paired F0 mice at day 42 (Student's unpaired t-test. 42d unpaired vs. paired P=0.2248. n=10,11.). Squares indicate males, triangles indicate females. **(F)** The approach-avoid indices of unpaired and paired F0 mice at day 63 (Student's unpaired t-test. 63d unpaired vs paired P=0.8987. n=6,8.).

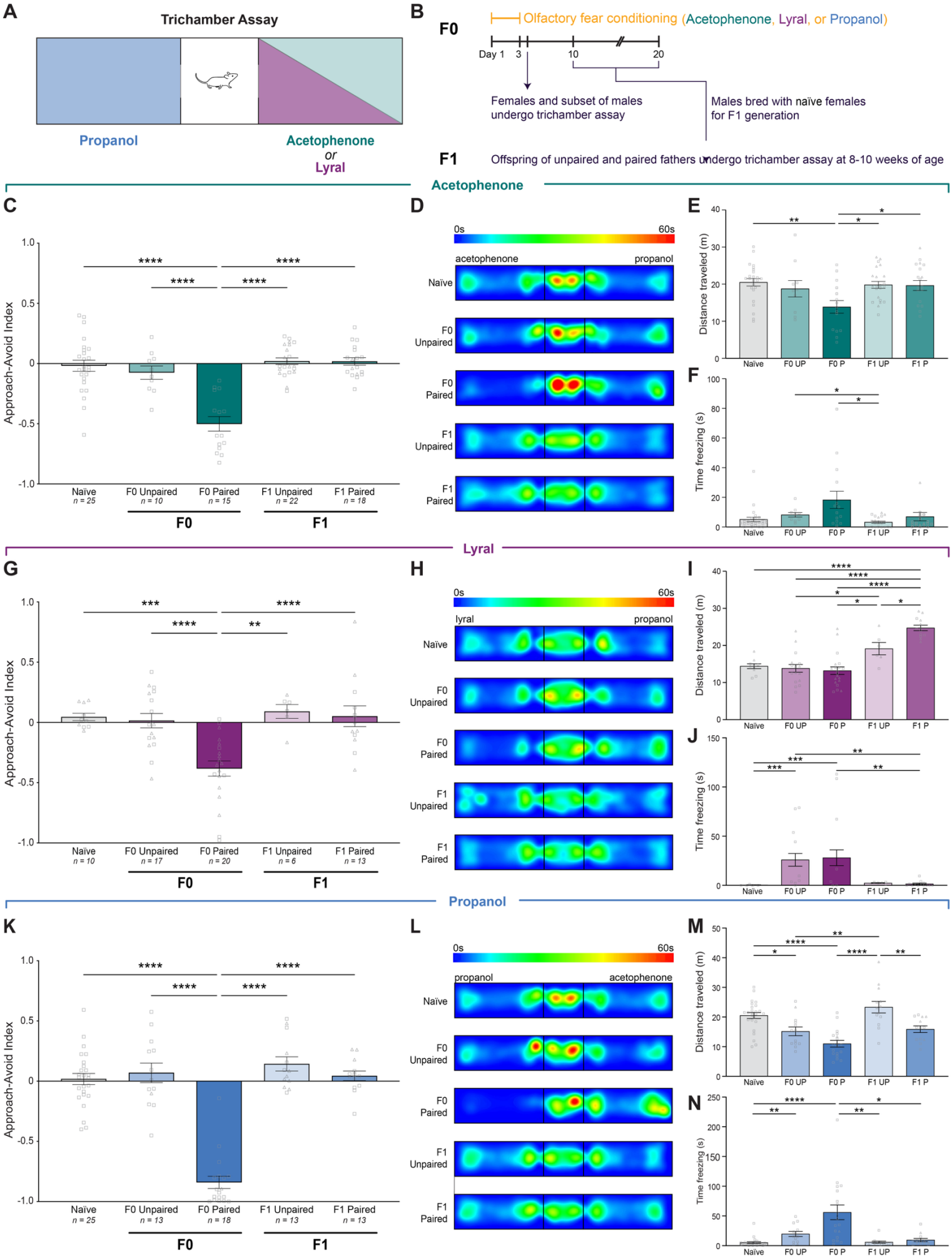
A
Trichamber Assay
Propanol
Acetophenone
or
Lyral
B
F0
Olfactory fear conditioning (Acetophenone, Lyral, or Propanol)
Day 1
3
10
20
Females and subset of males
undergo trichamber assay
Males bred with naïve females
for F1 generation
F1
Offspring of unpaired and paired fathers undergo trichamber assay at 8-10 weeks of age
Acetophenone
C
Approach-Avoid Index
Naïve
n = 25
F0 Unpaired
n = 10
F0 Paired
n = 15
F1 Unpaired
n = 22
F1 Paired
n = 18
F0
F1
D
0s
60s
acetophenone
propanol
Naïve
F0
Unpaired
F0
Paired
F1
Unpaired
F1
Paired
E
Distance traveled (m)
Naïve
F0 UP
F0 P
F1 UP
F1 P
F
Time freezing (s)
Lyral
G
Approach-Avoid Index
Naïve
n = 10
F0 Unpaired
n = 17
F0 Paired
n = 20
F1 Unpaired
n = 6
F1 Paired
n = 13
F0
F1
H
0s
60s
lyral
propanol
Naïve
F0
Unpaired
F0
Paired
F1
Unpaired
F1
Paired
I
Distance traveled (m)
Naïve
F0 UP
F0 P
F1 UP
F1 P
J
Time freezing (s)
Propanol
K
Approach-Avoid Index
Naïve
n = 25
F0 Unpaired
n = 13
F0 Paired
n = 18
F1 Unpaired
n = 13
F1 Paired
n = 13
F0
F1
L
0s
60s
propanol
acetophenone
Naïve
F0
Unpaired
F0
Paired
F1
Unpaired
F1
Paired
M
Distance traveled (m)
Naïve
F0 UP
F0 P
F1 UP
F1 P
N
Time freezing (s)

Fig. 5. Olfactory fear conditioning leads to nuanced behavioral differences in F1 offspring. **(A)** Schematic of the trichamber assay showing the three conditioning odors and control odors. Propanol was the control odor for acetophenone and lyral, and acetophenone was the control odor for propanol. **(B)** Timeline of olfactory fear conditioning, behavior testing in F0, F0 breeding for the F1 generation, and F1 behavior testing. Conditioned F0 males used to breed for F1s did not undergo behavioral testing to prevent any extinction effects. **(C)** The approach-avoid indices of acetophenone-conditioned naïve, unpaired, and paired F0 mice, and F1 mice bred from unpaired and paired F0 fathers (One-way ANOVA. P<0.0001. Tukey's multiple comparisons. Naïve vs. F0 Paired P<0.0001. F0 Unpaired vs. F0 Paired P<0.0001. F0 Paired vs. F1 Unpaired P<0.0001. F0 Paired vs. F1 Paired P<0.0001. n=25,10,15,22,18.). Squares indicate males, triangles indicate females. **(D)** Group-averaged heat maps for acetophenone-conditioned F0 mice and F1 offspring, with the acetophenone chamber on the left and the control (propanol) chamber on the right. **(E)** Distance traveled in the trichamber assay for acetophenone-conditioned F0 mice and F1 offspring (One-way ANOVA. P=0.0041. Tukey's multiple comparisons. Naïve vs. F0 Paired P=0.0032. F0 Paired vs. F1 Unpaired P=0.0141. F0 Paired vs. F1 Paired P=0.0103. n=25,10,15,22,18). **(F)** Time freezing for acetophenone-conditioned F0 mice and F1 offspring (Kruskal-Wallis test. P=0.0022. Dunn's multiple comparisons. F0 Unpaired vs. F1 Unpaired P=0.0406. F0 Paired vs. F1 Unpaired P=0.0262. n=25,10,15,22,18.). **(G)** The approach-avoid indices of lyral-conditioned naïve, unpaired, and paired F0 mice, and F1 mice bred from unpaired and paired F0 fathers (One-way ANOVA. P<0.0001. Tukey's multiple comparisons. Naïve vs. F0 Paired P=0.0004. F0 Unpaired vs. F0 Paired P<0.0001. F0 Paired vs. F1 Unpaired P=0.0013. F0 Paired vs. F1 Paired P<0.0001. n=10,17,20,6,13.). **(H)** Group-averaged heat maps for lyral-conditioned F0 mice and F1 offspring, with the lyral chamber on the left and the control (propanol) chamber on the right. **(I)** Distance traveled in the trichamber assay for lyral-conditioned F0 mice and F1 offspring (One-way ANOVA. P<0.0001. Tukey's multiple comparisons. Naïve vs. F1 Paired P<0.0001. F0 Unpaired vs. F1 Unpaired P=0.037. F0 Unpaired vs. F1 Paired P<0.0001. F0 Paired vs. F1 Unpaired P=0.0121. F0 Paired vs. F1 Paired P<0.0001. F1 Unpaired vs. F1 Paired P=0.0325. n=10,17,20,6,13.). **(J)** Time freezing for lyral-conditioned F0 mice and F1 offspring (Kruskal-Wallis test. P<0.0001. Dunn's multiple comparisons. Naïve vs. F0 Unpaired P=0.0001. Naïve vs. F0 Paired P=0.0005. F0 Unpaired vs. F1 Paired P=0.0012. F0 Paired vs. F1 Paired 0.0041. n=10,17,20,6,13.). **(K)** The approach-avoid indices of propanol-conditioned naïve, unpaired, and paired F0 mice, and F1 mice bred from unpaired and paired F0 fathers (One-way ANOVA. P<0.0001. Tukey's multiple comparisons. Naïve vs. F0 Paired P<0.0001. F0 Unpaired vs. F0 Paired P<0.0001. F0 Paired vs. F1 Unpaired P<0.0001. F0 Paired vs. F1 Paired P<0.0001. n=25,13,18,13,13.). **(L)** Group-averaged heat maps for propanol-conditioned F0 mice and F1 offspring, with the propanol chamber on the left and the control (acetophenone) chamber on the right. **(M)** Distance traveled in the trichamber assay for propanol-conditioned F0 mice and F1 offspring (One-way ANOVA. P<0.0001. Tukey's multiple comparisons. Naïve vs. F0 Unpaired P=0.0304. Naïve vs. F0 Paired P<0.0001. F0 Unpaired vs. F1 Unpaired P=0.0014. F0 Paired vs. F1 Unpaired P<0.0001. F1 Unpaired vs. F1 Paired P=0.0045. n=25,13,18,13,13.). **(N)** Time

freezing for propanol-conditioned F0 mice and F1 offspring (Kruskal-Wallis test. $P<0.0001$. Dunn's multiple comparisons. Naïve vs. F0 Unpaired $P=0.0074$. Naïve vs. F0 Paired $P<0.0001$. F0 Paired vs. F1 Unpaired $P=0.0011$. F0 Paired vs. F1 Paired $P=0.028$. n=25,13,18,13,13.).

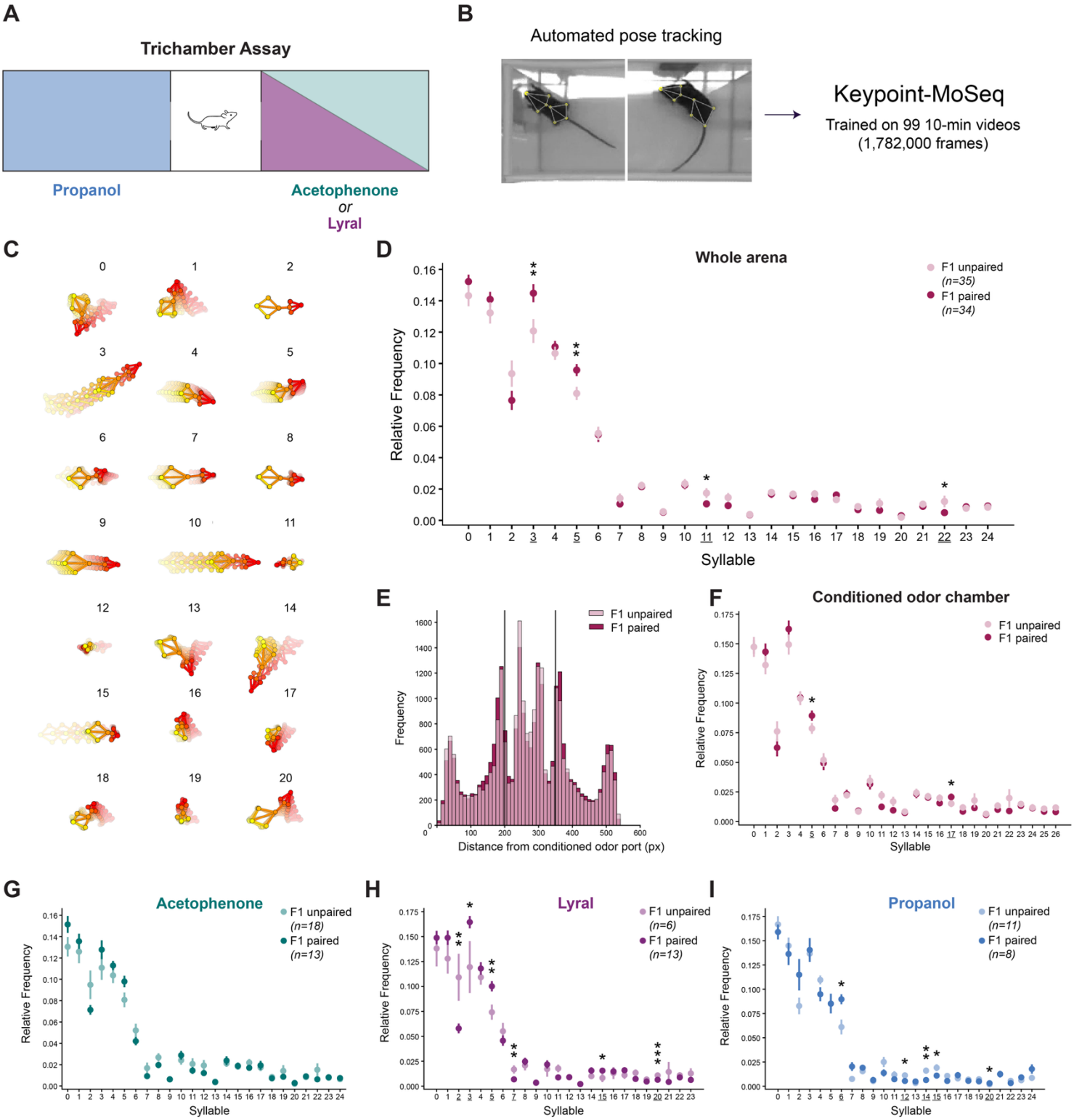

830 **Fig. 6. Unsupervised machine learning analysis identifies behavioral differences in F1. (A)** Schematic of the trichamber assay showing the three conditioning odors and control odors. Propanol was the control odor for acetophenone and lyral, and acetophenone was the control odor

for propanol. **(B)** Analysis pipeline for Keypoint-MoSeq. Eight keypoints were tracked across the entire 10-minute trichamber assay for 99 videos, and the tracking data was used to train a Keypoint-MoSeq model. **(C)** Trajectory plots of the 21 most frequently used syllables across the dataset. **(D)** The relative usage frequencies of syllables in the whole trichamber arena in the F1 offspring of unpaired (light pink) and paired (dark pink) fathers. Syllables with significantly different usage between groups are underlined in the x-axis and denoted with asterisks above the data points (Kruskal-Wallis test with Dunn's multiple comparisons. Syllable 3 F1 unpaired vs. F1 paired P=0.00696. Syllable 5 P=0.0054. Syllable 11 P=0.02505. Syllable 22 P=0.0184. n=35,34.). **(E)** Histogram of the frequency (number of observations divided by the bin width) of each animal's center point along the x-axis (x distance from the conditioned odor port). The two vertical bars indicate the divisions between the three chambers (conditioned odor chamber left, control odor chamber right). **(F)** The relative usage frequencies of syllables in the conditioned odor chamber in F1 unpaired (light pink) and F1 paired (dark pink) (Kruskal-Wallis test with Dunn's multiple comparisons. Syllable 5 F1 unpaired vs. F1 paired P=0.0406. Syllable 17 P=0.046695. n=35,34.). **(G)** The relative usage frequencies of syllables in the whole arena in the F1 offspring of acetophenone-unpaired (light green) and acetophenone-paired (dark green) fathers (n=18.13.). **(H)** The relative usage frequencies of syllables in the whole arena in the F1 offspring of lyral-unpaired (light purple) and lyral-paired (dark purple) fathers (Kruskal-Wallis test with Dunn's multiple comparisons. Syllable 2 lyral F1 unpaired vs. F1 paired P=0.0016. Syllable 3 P=0.02724. Syllable 5 P=0.003. Syllable 7 P=0.00252. Syllable 15 P=0.0208. Syllable 20 P=0.00015. n=6,13.). **(I)** The relative usage frequencies of syllables in the whole arena in the F1 offspring of propanol-unpaired (light blue) and propanol-paired (dark blue) fathers (Kruskal-Wallis test with Dunn's multiple comparisons. Syllable 6 propanol F1 unpaired vs. F1 paired P=0.0206. Syllable 12 P=0.04068. Syllable 14 P=0.0072. Syllable 15 P=0.03204. Syllable 20 P=0.0148. n=11,8.).

Materials and Methods

Mice

All procedures were approved by the Columbia University Institutional Animal Care and Use Committee under protocol #AABL8552. All mice were housed with a 12-hour light/12-hour dark cycle and fed ad libitum. M71-IRES-tauGFP (Stock #006676), MOR23-IRES-tauGFP (Stock #006643), and C57BL/6J (Stock #000664) mice were obtained from The Jackson Laboratory or gifted from the Lomvardas and the Axel laboratories. The M71-IRES-tauRFP2 line was generated in-house.

Transgenic mouse line

The M71-IRES-tauRFP2 mouse line was generated by homologous recombination of mouse ES cells using established techniques. Briefly, the targeting vector (Addgene 15510) was linearized using PmeI and electroporated into MM13 ES cells (129S/SvEv). Targeted ES clones were identified by Southern blot hybridization and positive ES cells were transferred into C57BL/6 blastocysts. Male chimeras were bred with C57BL/6 females to establish germline transmission and subsequently outcrossed to C57BL/6 females for at least 5 generations. Deletion of the self-excising Neo cassette was confirmed by PCR of genomic DNA.

Olfactory fear conditioning

8–12-week-old male and female mice were trained to associate acetophenone (Sigma-Aldrich, 42163), lyral (IFF, 00129214), or propanol (Sigma-Aldrich, I9516) with 0.75mA foot shocks. Odors were diluted to 10% v/v in mineral oil (Fisher, O121-1). The mice were trained on 3 consecutive days, with each training day consisting of 5 presentations of odor for 10 seconds. For mice in the paired condition, the odor presentations were co-terminated with a 0.75mA foot shock. For mice in the unpaired condition, there was a 60-second delay between the odor presentation and foot shock (Fig 1C.). Olfactory fear conditioning boxes, olfactometers, and software were obtained from Med Associates. Mice were randomly assigned to experimental conditions.

Tissue clearing

MOEs were perfused, dissected, and processed according to the iDISCO+ protocol (Renier et al. 2016). Whole MOEs were processed in 5mL volumes. Samples were postfixed in 4% paraformaldehyde in 1X PBS (Electron Microscopy Sciences, 15710-S) overnight at 4°C. The following day, they were washed with 1X PBS (3 x 30 minutes), gradually dehydrated with methanol (MeOH; Sigma-Aldrich, 322415) over 5 hours, and incubated in 66% dichloromethane (DCM; Sigma-Aldrich, 270997)/33% MeOH overnight. The samples were washed in 100% MeOH the following day, chilled at 4°C, bleached in 5% hydrogen peroxide (Sigma-Aldrich, 216763) in MeOH overnight at 4°C, and then gradually rehydrated the next day. Samples were permeabilized for 2 days and blocked in 6% goat serum (Jackson ImmunoResearch, 005-000-121) for 2 days at 37°C. Next, they were labeled with a 1:2000 dilution of primary chicken anti-GFP antibody (Aves Labs, GFP-1020) for 3 days at 37°C, washed for 1 day (5 x 1 hour), and labeled with a 1:1000 dilution of secondary goat anti-chicken Alexa Fluor 647 antibody (Invitrogen, A-21449) for 3 days at 37°C. Due to the fragility of the nasal turbinates housing the majority of zone 1, samples were embedded in 4% agarose (Invitrogen, 16500100) prior to final dehydration (Fig 1E.). Lastly, the embedded samples were incubated in 66% DCM/33% MeOH for 3 hours, rinsed

twice with 100% DCM, and transferred to dibenzyl ether (Sigma-Aldrich, 33630) for final clearing.

Light sheet imaging

Images were collected with a light-sheet microscope (Ultramicroscope II, LaVision BioTec) at 2.0X magnification using a 640 nm laser and a z-step size of 2.0µm. All cleared tissue images were acquired with tissue submerged in dibenzyl ether (DBE). Laser intensity was set between 55% and 75% to prevent oversaturated pixels and photobleaching. The working distance of the microscope allowed for complete visualization of both left and right turbinates containing zone 1 OSNs (Fig. 1F, H.). The light-sheet microscope was provided by Cellular Imaging at the Zuckerman Institute (NIH 1S10OD023587-01).

Imaris 3D cell quantification

All quantification was performed in a double-blind manner. The image stack of GFP+ olfactory sensory neurons in the 647 nm channel was analyzed using Imaris software. The average number of olfactory sensory neurons was measured using the spot detection tool on 350^3 μm^3 cubes of zone 1 tissue, with a requirement of at least 3 cubes per sample for inclusion. The decision to measure an average number of cells within a fixed volume, as opposed to the total number of cells in the turbinates, accounted for potential tissue loss and differences in tissue volumes/shapes across samples. The spot detection was set to a 16.3µm estimated diameter and was based on Imaris' quality threshold, which compares the intensities at the centers of the candidate spots. The quality threshold varied slightly across samples to adjust for signal quality and axon brightness (to minimize counting spots on axons) but was held consistent within every sample.

5-Ethynyl-2′-deoxyuridine (EdU) injections

10mM EdU (Invitrogen, E10187) was administered to male and female 8–12-week-old M71-$GFP^{+/+}$ and MOR23-$GFP^{+/+}$ mice through a series of daily 0.01mL/g intraperitoneal injections. Injections were administered 15 minutes prior to olfactory fear conditioning on each of the 3 days of conditioning, plus 2 additional days around the same time conditioning had been performed (Fig 3A.).

EdU click chemistry

Mice were transcardially perfused with ice-cold 4% PFA (Electron Microscopy Sciences, 15710-S) in 1X PBS. MOEs were surgically dissected, incubated in 4% PFA overnight, and cryoprotected in 30% sucrose (Sigma-Aldrich, S0389). MOEs were frozen in OCT (Fisher, 23-730-571) and stored at -20°C until sectioning. Tissue was sliced into 20µm sections, mounted directly onto Fisher Superfrost Plus glass slides (Fisher, 12-550-15), and stored at -80°C until staining. At the time of staining, slides were acclimated to room temperature, washed with PBST (0.1% Triton X-100 in 1X PBS; 3 x 5 minutes; Sigma-Aldrich, X100), and incubated with Click-iT Plus EdU reaction cocktail (Alexa Fluor 555; 30 minutes; Invitrogen, C10638). Sections were washed again with PBST (3 x 5 minutes), with the last wash including 1:10,000 DAPI (Invitrogen, D1306), and then cover-slipped using Vectashield Plus mounting medium (Vector Labs H-1900) and sealed with nail polish.

Confocal image acquisition

Slides were imaged using a Zeiss Upright LSM 880 Confocal microscope and Zen Black software (Zeiss) or W1-Yokogawa Spinning Disk Confocal (Nikon). All co-labeling images were acquired in z-stacks to ensure accuracy in co-labeling determination.

Trichamber assay

At least 1 day following olfactory fear conditioning, conditioned mice were assayed in a custom-built acrylic three-chamber box to assess odor avoidance behavior (Fig 4.). The conditioned and control odors were assigned randomly to either side. Odors were diluted to 1% v/v in mineral oil for all odor preference assays, and flowmeters were set to equal flow rates of approximately 1 liter/minute. The three-chamber box included vacuum ports both in the center chamber, as well as on either side of the center chamber doorways in the side chambers to ensure that each experimental odor was restricted to its chamber. The mice were habituated to the center chamber for 1 minute prior to the start of the test, and then the doors to both chambers were lifted to initiate the assay. Mice were recorded roaming freely throughout the three-chamber box for 10 minutes.

Behavioral analysis

We used ANY-maze software to track the position of the mice throughout the entire trichamber trial. The odor avoidance index was calculated as approach-avoidance index = (time spent on control odor side - time spent on conditioned odor side) / total time spent on either side. Animals visibly sampled each chamber to be included in analysis. We also used ANY-maze to generate heat maps and determine distance traveled, time freezing, and mean speed metrics during the assay. For pose estimation, we trained a SLEAP model (Pereira et al., 2022) to track eight keypoints (nose, right ear, left ear, neck, center, right leg, left leg, tailbase) on each mouse across each 10-minute trial. With tracking data from 99 (30 F0, 69 F1) 10-minute trichamber videos that were all recorded by the same camera and in the same apparatus, we trained a Keypoint-MoSeq model (Weinreb et al., 2024) to identify behavioral syllables. The model had 6 latent dimensions (explaining >90% of the variance) and a kappa value of 1e6. For statistical analyses, a minimum relative frequency cutoff of 0.005 was applied for syllables.

Statistics

A significance threshold of $p<0.05$ was used for all statistical analyses. Outlier tests were performed on all data, leading to the removal of one statistical outlier from the Acetophenone F1 Paired group. This outlier was also excluded from analyses of other metrics from the same behavioral assay. After performing Shapiro-Wilk normality tests, normally distributed data across 2+ groups were performed using a standard one-way ANOVA with Tukey's multiple comparisons post-hoc tests. Normally distributed data between 2 groups were performed using Student's unpaired t-tests. For data that was not normally distributed, 2+ groups were analyzed with a nonparametric one-way ANOVA (Kruskal-Wallis test) and Dunn's multiple comparisons post-hoc tests. Descriptive statistics used standard error of the mean (S.E.M.) to estimate error. Percent differences between 2 groups were calculated by comparing the mean of each group. For all analysis except Keypoint-MoSeq, statistical analysis was performed using Prism 9 (GraphPad) software. For Keypoint-Moseq statistics, a combination of Keypoint-MoSeq code and custom Python code was used for statistical analysis.

\

Supplementary Figures

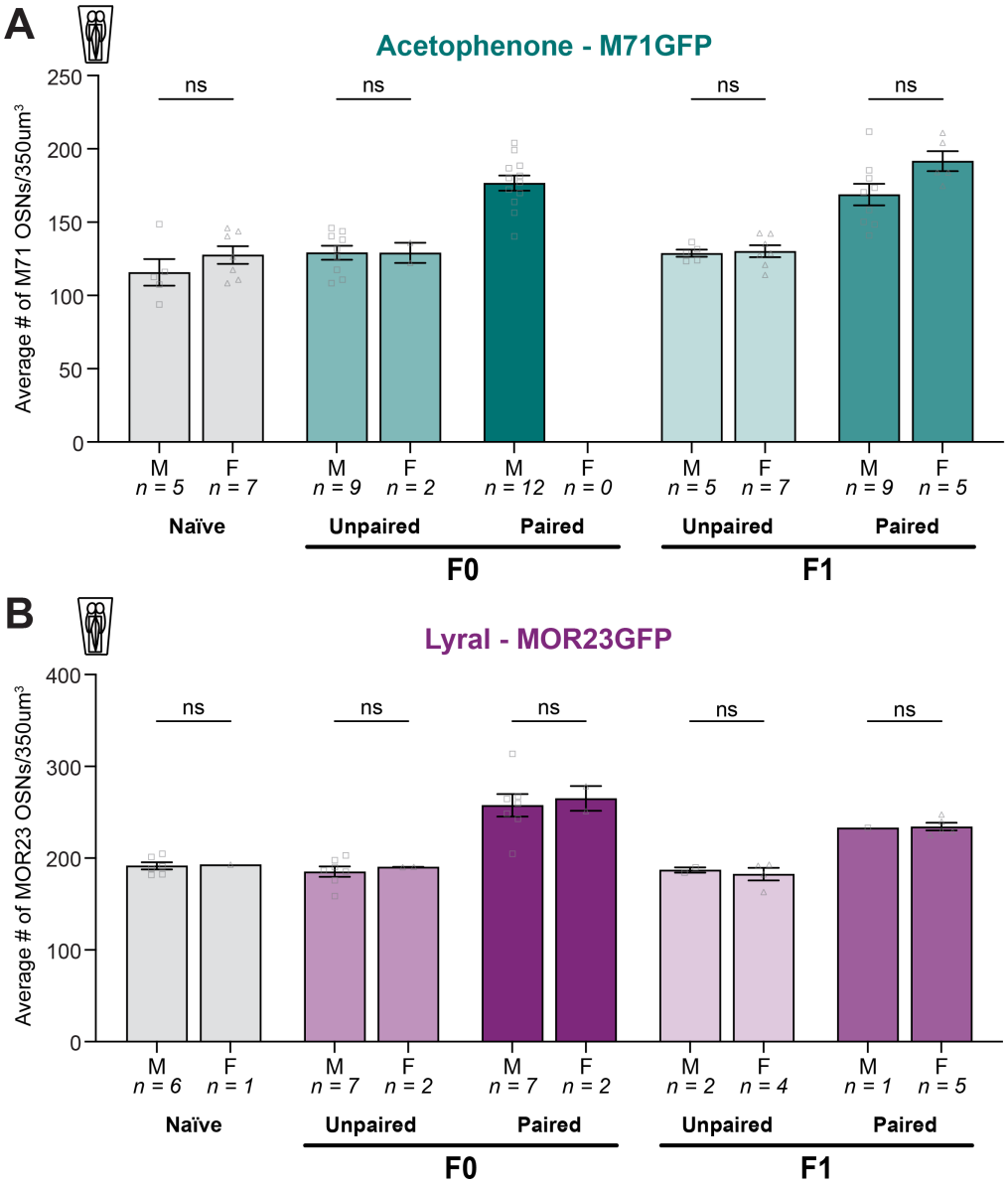

Fig. S1. Conditioned odor-responsive OSN counts by sex. (A) The average number of M71 OSNs in a 350^3 μm^3 cube of epithelium of naïve (gray), acetophenone unpaired (lighter green), and acetophenone paired (darker green) conditions in F0 and F1, separated by sex (Two-way ANOVA. Treatment factor P<0.0001. Sex factor P=0.0425. n=5,7,9,2,12,0,5,7,9,5.). **(B)** The average number of MOR23 OSNs in a 350^3 μm^3 cube of epithelium of naïve (gray), lyral unpaired (lighter purple), and lyral paired (darker purple) conditions in F0 and F1, separated by sex (Two-way ANOVA. Treatment factor P<0.0001. Sex factor P=0.7206. n=6,1,7,2,7,2,2,4,1,5.).

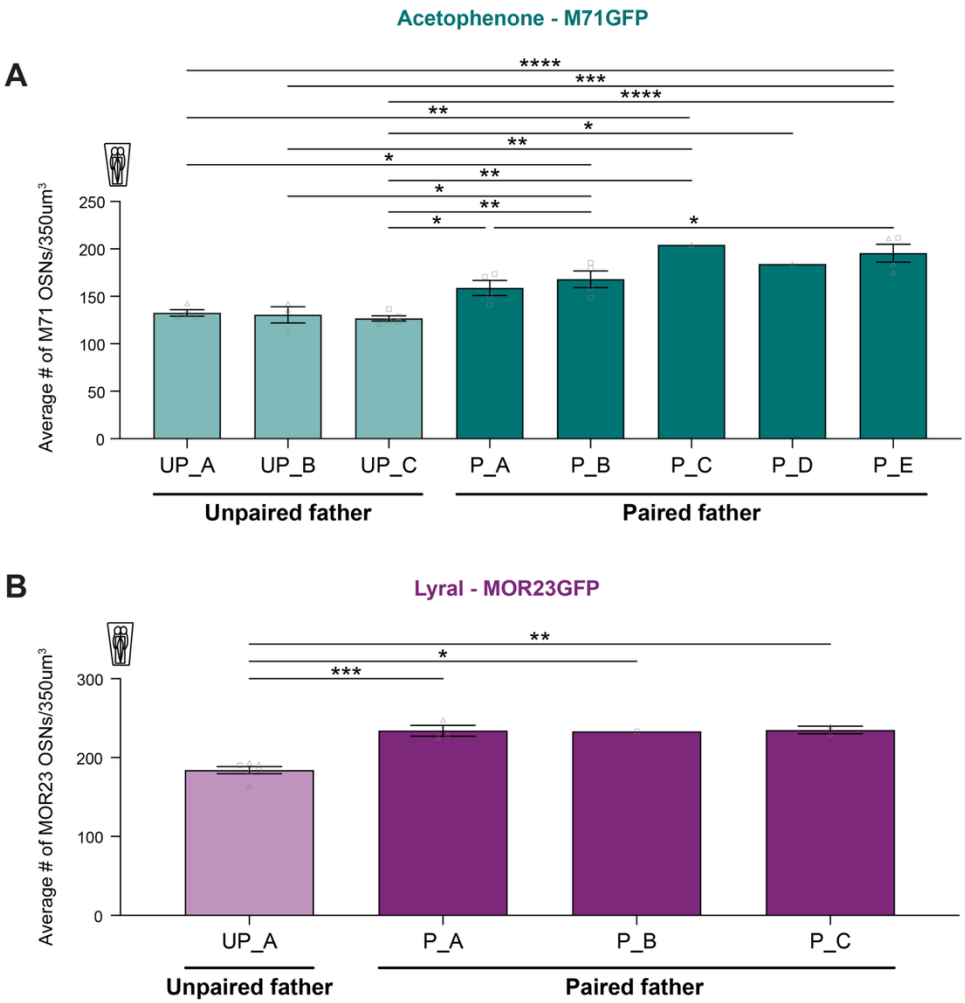

Fig. S2. F1 conditioned odor-responsive OSN counts by litter. (A) The average number of M71 OSNs in a 350^3 μm^3 cube of epithelium of the F1 offspring of acetophenone-unpaired (lighter green), and acetophenone-paired (darker green) fathers, separated by litter (One-way ANOVA. P<0.0001. Tukey's multiple comparisons. UP_A vs. P_B P=0.0329. UP_A vs. P_C P=0.0041. UP_A vs. P_E P=0.0001. UP_B vs. P_B P=0.038. UP_B vs. P_C P=0.0043. UP_B vs. P_E P=0.0002. UP_C vs. P_A P=0.046. UP_C vs. P_B P=0.006. UP_C vs. P_C P=0.0015. UP_C vs. P_D P=0.0241. UP_C vs. P_E P<0.0001. P_A vs. P_E P=0.0257. n=4,3,5,4,4,1,1,4.). **(B)** The average number of MOR23 OSNs in a 350^3 μm^3 cube of epithelium of the F1 offspring of lyral-unpaired (lighter green), and lyral-paired (darker green) fathers, separated by litter (One-way ANOVA. P=0.0004. UP_A vs. P_A P=0.0008. UP_A vs. P_B P=0.0133. UP_A vs. P_C P=0.002. n=6,3,1,2.).

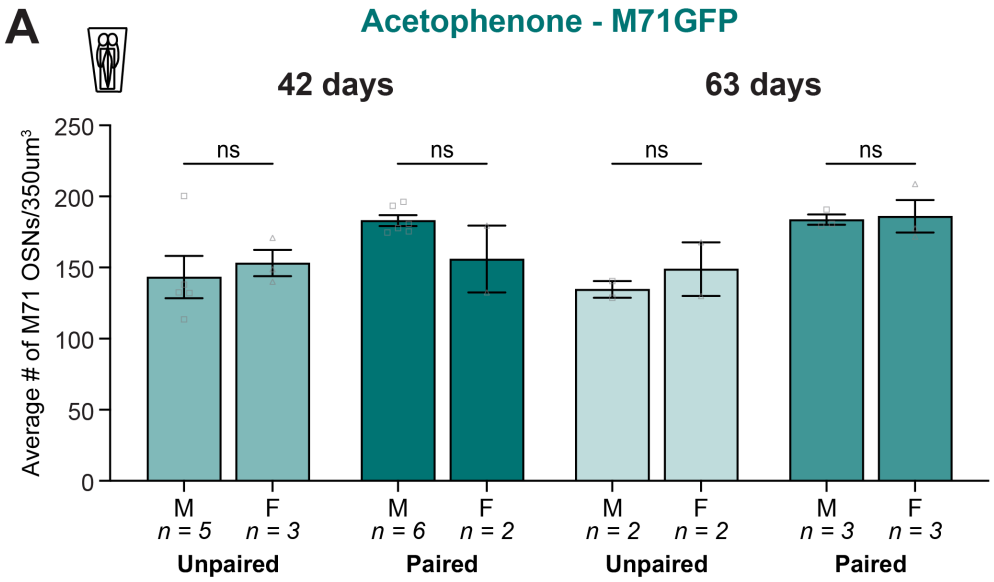

Fig. S3. Extended timepoint OSN counts by sex. (A) The average number of M71 OSNs in a 350^3 μm^3 cube of epithelium of unpaired (light green) and paired (dark green) mice, 42- or 63-days post-conditioning, separated by sex (Two-way ANOVA. Treatment factor P=0.0123. Sex factor P=0.9889. n=5,3,6,2,2,2,3,3.).

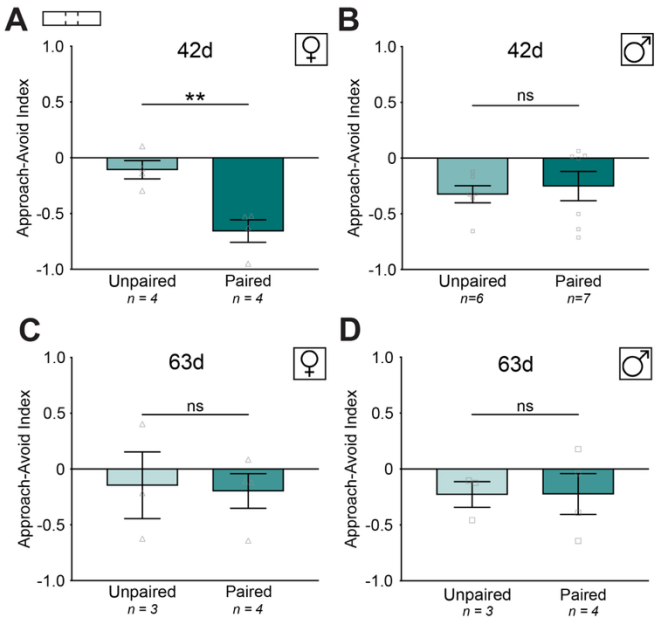

Fig. S4. Extended timepoint trichamber assay by sex. (A) The approach-avoid indices of female unpaired and paired F0 mice at day 42 (Student's unpaired t-test. P=0.0055. n=4,4.). **(B)** The approach-avoid indices of male unpaired and paired F0 mice at day 42 (Student's unpaired t-test. P=0.6534. n=6,7.). **(C)** The approach-avoid indices of female unpaired and paired F0 mice at day 63 (Student's unpaired t-test. P=0.8762. n=3,4.). **(D)** The approach-avoid indices of male unpaired and paired F0 mice at day 63 (Student's unpaired t-test. P=0.9859. n=3,4.).

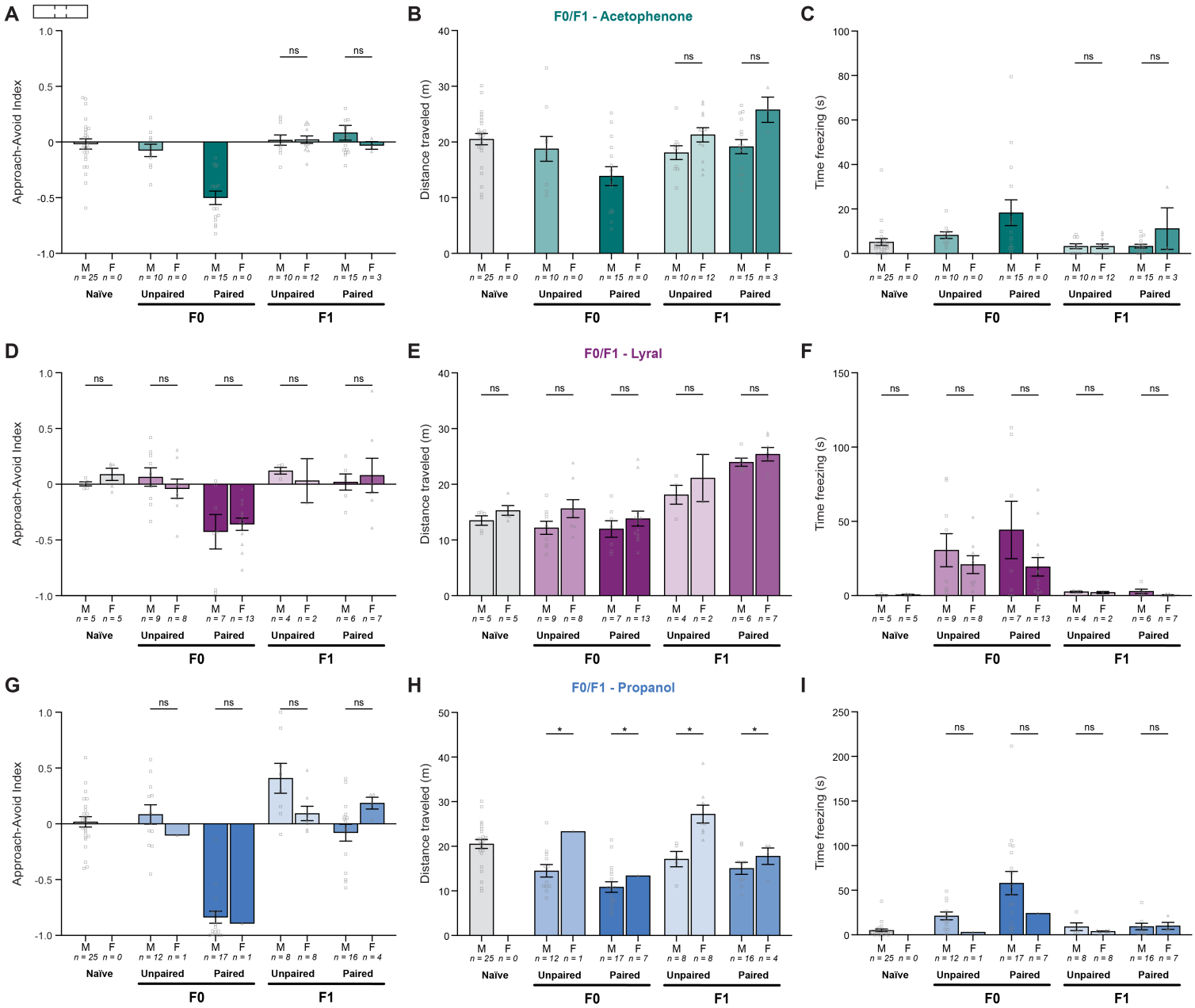

Fig. S5. Trichamber assay metrics by sex. (A) The approach-avoid indices of acetophenone-conditioned naïve, unpaired, and paired F0 mice, and F1 mice bred from unpaired and paired F0 fathers, separated by sex (Two-way ANOVA. Treatment factor P<0.0001. Sex factor P=0.8137. n=25,0,10,0,15,0,10,12,15,3.). **(B)** Distance traveled in the trichamber assay for acetophenone-conditioned F0 mice and F1 offspring, separated by sex (Two-way ANOVA. Treatment factor P=0.0049. Sex factor P=0.0261. n=25,0,10,0,15,0,10,12,15,3.). **(C)** Time freezing for acetophenone-conditioned F0 mice and F1 offspring, separated by sex (Two-way ANOVA. Treatment factor P=0.0008. Sex factor P=0.5149. n=25,0,10,0,15,0,10,12,15,3.). **(D)** The approach-avoid indices of lyral-conditioned naïve, unpaired, and paired F0 mice, and F1 mice bred from unpaired and paired F0 fathers, separated by sex (Two-way ANOVA. Treatment factor P<0.0001. Sex factor P=0.9573. n=5,5,9,8,7,13,4,2,6,7.). **(E)** Distance traveled in the trichamber assay for lyral-conditioned F0 mice and F1 offspring, separated by sex (Two-way

ANOVA. Treatment factor P<0.0001. Sex factor P=0.016. n=5,5,9,8,7,13,4,2,6,7.). **(F)** Time freezing for lyral-conditioned F0 mice and F1 offspring, separated by sex (Two-way ANOVA. Treatment factor P=0.0013. Sex factor P=0.0938. n=5,5,9,8,7,13,4,2,6,7.). **(G)** The approach-avoid indices of propanol-conditioned naïve, unpaired, and paired F0 mice, and F1 mice bred from unpaired and paired F0 fathers, separated by sex (Two-way ANOVA. Treatment factor P<0.0001. Sex factor P=0.4375. n=25,0,12,1,17,1,8,8,16,4.). **(H)** Distance traveled in the trichamber assay for propanol-conditioned F0 mice and F1 offspring, separated by sex (Two-way ANOVA. Treatment factor P<0.0001. Sex factor P=0.0005. Tukey's multiple comparisons. F0 Unpaired male vs. female P= 0.0165. F0 Paired male vs. female P=0.0165. F1 Unpaired male vs. female P=0.0165. F1 Paired male vs. female P=0.0165. n=25,0,12,1,17,1,8,8,16,4.). **(I)** Time freezing for propanol-conditioned F0 mice and F1 offspring, separated by sex (Two-way ANOVA. Treatment factor P<0.0001. Sex factor P=0.3945. n=25,0,12,1,17,1,8,8,16,4.).

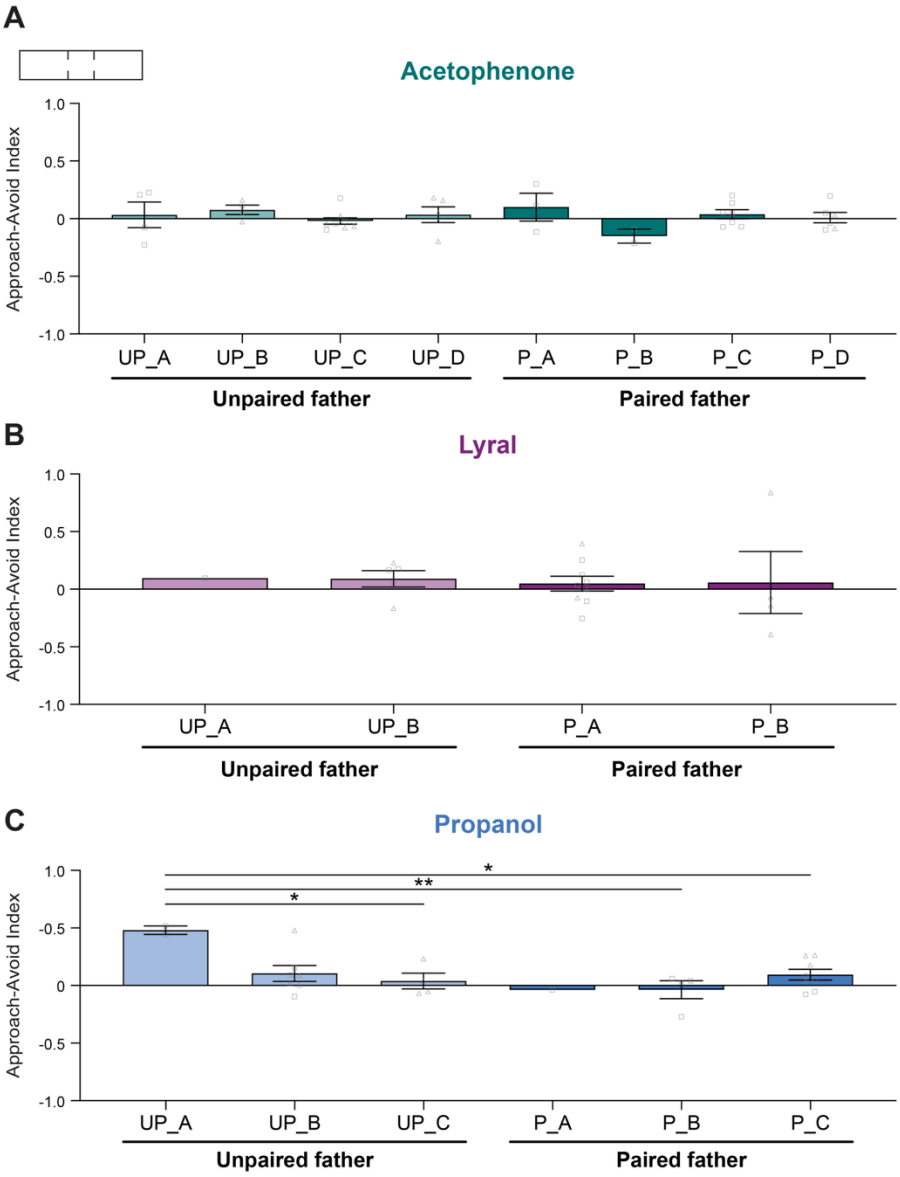

Fig. S6. Trichamber assay avoidance index by litter. (A) The approach-avoid indices of acetophenone-conditioned naïve, unpaired, and paired F0 mice, and F1 mice bred from unpaired and paired F0 fathers, separated by litter (One-way ANOVA. P=0.487. n=4,4,9,5,3,2,7,6.). **(B)** The approach-avoid indices of lyral-conditioned naïve, unpaired, and paired F0 mice, and F1 mice bred from unpaired and paired F0 fathers, separated by litter (One-way ANOVA. P=0.9939. n=1,5,9,4.). **(C)** The approach-avoid indices of propanol-conditioned naïve, unpaired, and paired F0 mice, and F1 mice bred from unpaired and paired F0 fathers, separated by litter (One-way ANOVA. P=0.0199. Tukey's multiple comparisons. UP_A vs. UP_C P=0.0306. UP_A vs. P_B P=0.0088. UP_A vs. P_C P=0.041. n=2,7,4,1,4,8.).

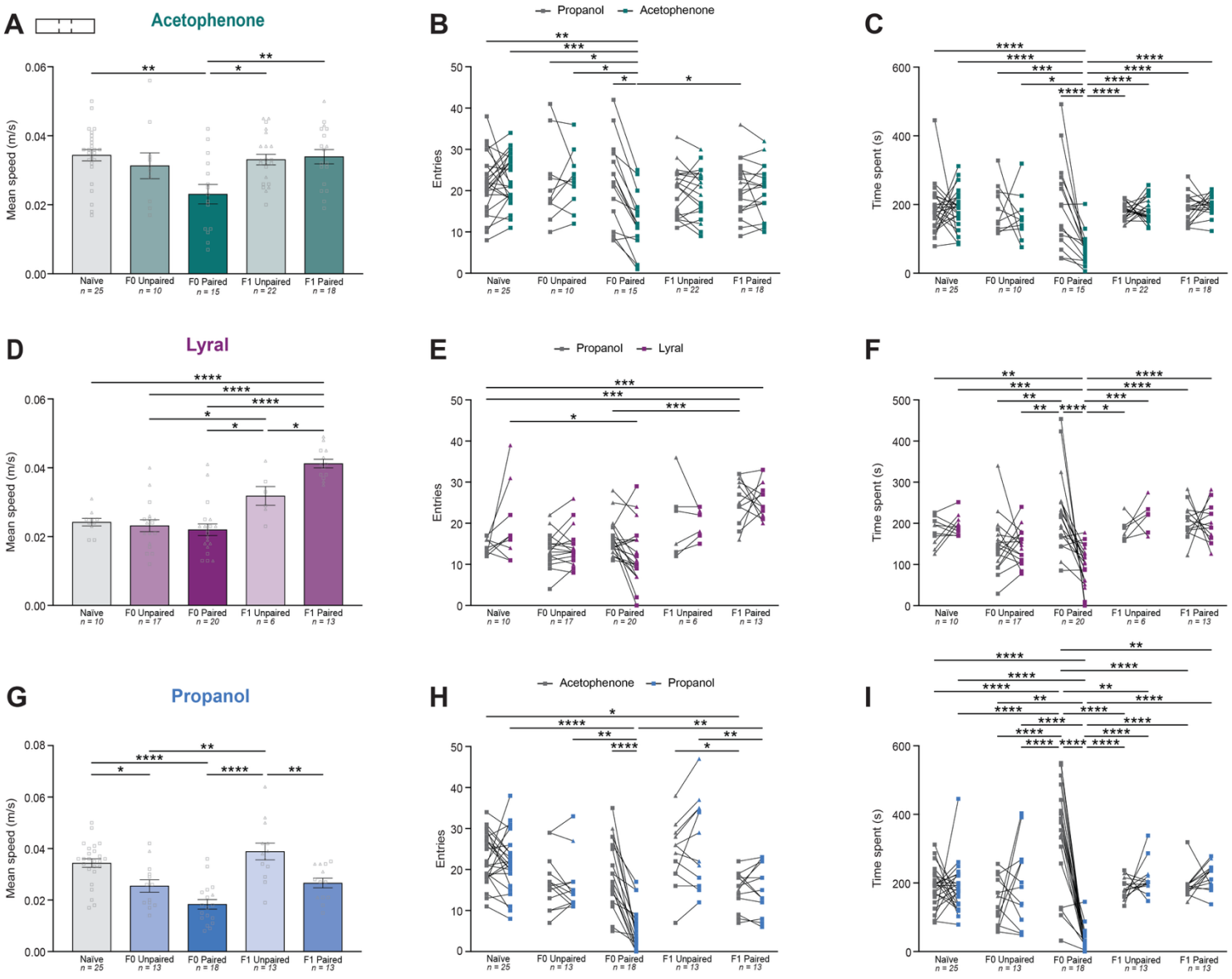

Fig. S7. Additional trichamber assay metrics. (A) The mean speed of acetophenone-conditioned naïve, unpaired, and paired F0 mice, and F1 mice bred from unpaired and paired F0 fathers (One-way ANOVA. P=0.003. Tukey's multiple comparisons. Naïve vs. F0 Paired P=0.0024. F0 Paired vs. F1 Unpaired P=0.0121. F0 Paired vs. F1 Paired P=0.0081. n=25,10,15,22,18.). **(B)** The number of entries into the propanol (control) and acetophenone (conditioned odor) chambers in naïve, unpaired, and paired F0 mice, and F1 mice bred from unpaired and paired F0 fathers (Two-way ANOVA. Treatment factor P=0.0174. Odor factor P=0.1339. P-values from Tukey's multiple comparisons tests in Table S2.7. n=25,10,15,22,18.). **(C)** Time spent in the propanol (control) and acetophenone (conditioned odor) chambers in naïve, unpaired, and paired F0 mice, and F1 mice bred from unpaired and paired F0 fathers (Two-way ANOVA. Treatment factor P=0.0022. Odor factor P=0.0053. P-values from Tukey's multiple comparisons tests in Table S2.7. n=25,10,15,22,18.). **(D)** The mean speed of lyral-conditioned naïve, unpaired, and paired F0 mice, and F1 mice bred from unpaired and paired F0 fathers (One-way ANOVA. P<0.0001. Tukey's multiple comparisons. Naïve vs. F1 Paired P<0.0001. F0 Unpaired vs. F1 Unpaired P=0.0438. F0 Unpaired vs. F1 Paired P<0.0001. F0 Paired vs. F1 Unpaired P=0.0128. F0 Paired vs. F1 Paired P<0.0001. F1 Unpaired vs. F1 Paired

P=0.0315. n=10,17,20,6,13.). **(E)** The number of entries into the propanol (control) and lyral (conditioned odor) chambers in naïve, unpaired, and paired F0 mice, and F1 mice bred from unpaired and paired F0 fathers (Two-way ANOVA. Treatment factor P<0.0001. Odor factor P=0.6465. P-values from Tukey's multiple comparisons tests in Table S2.7. n=10,17,20,6,13.). **(F)** Time spent in the propanol (control) and lyral (conditioned odor) chambers in naïve, unpaired, and paired F0 mice, and F1 mice bred from unpaired and paired F0 fathers (Two-way ANOVA. Treatment factor P=0.0007. Odor factor P=0.0914. P-values from Tukey's multiple comparisons tests in Table S2.7. n=10,17,20,6,13.). **(G)** The mean speed of propanol-conditioned naïve, unpaired, and paired F0 mice, and F1 mice bred from unpaired and paired F0 fathers (One-way ANOVA. P<0.0001. Tukey's multiple comparisons. Naïve vs. F0 Unpaired P=0.0295. Naïve vs. F0 Paired P<0.0001. F0 Unpaired vs F1 Unpaired P=0.0017. F0 Paired vs. F1 Unpaired P<0.0001. F1 Unpaired vs. F1 Paired P=0.0051. n=25,13,18,13,13.). **(H)** The number of entries into the acetophenone (control) and propanol (conditioned odor) chambers in naïve, unpaired, and paired F0 mice, and F1 mice bred from unpaired and paired F0 fathers (Two-way ANOVA. Treatment factor P<0.0001. Odor factor P=0.0435. P-values from Tukey's multiple comparisons tests in Table S2.7. n=25,13,18,13,13.). **(I)** Time spent in the acetophenone (control) and propanol (conditioned odor) chambers in naïve, unpaired, and paired F0 mice, and F1 mice bred from unpaired and paired F0 fathers (Two-way ANOVA. Treatment factor P=0.4521. Odor factor P=0.0016. P-values from Tukey's multiple comparisons tests in Table S2.7. n=25,13,18,13,13.).

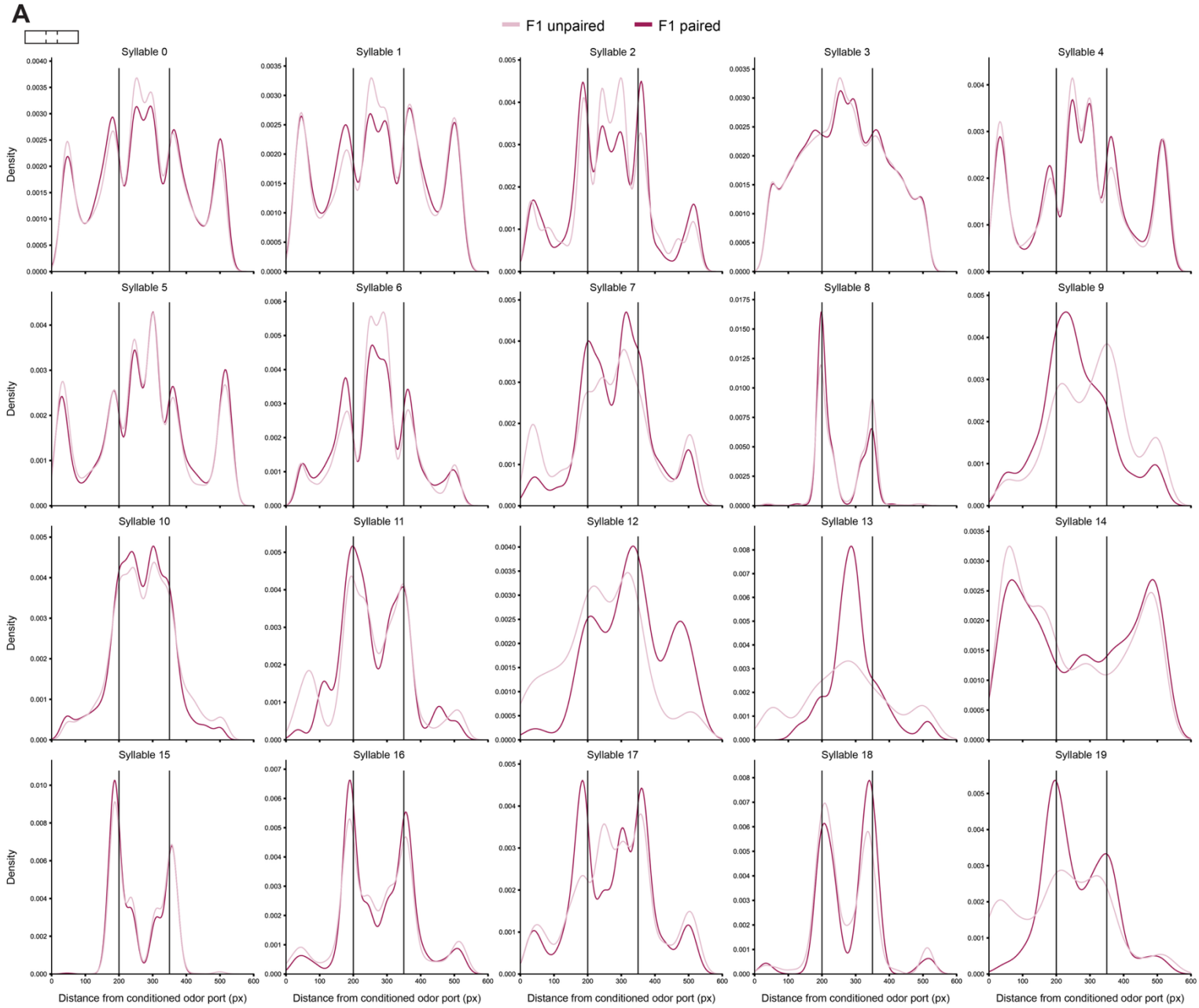

Fig. S8. Density of syllable usage across space in F1 offspring. (A) Kernel density estimate (KDE) plots of syllable usage as a function of the animal's center point along the x-axis (x distance from the conditioned odor port). The two vertical bars indicate the divisions between the three chambers (conditioned odor chamber left, control odor chamber right). n=35 (F1 unpaired), 34 (F1 paired).

Movie S1.

Representative videos of odor preference behavior assay. Left chamber: propanol. Right chamber: lyral. In the left video, the mouse has undergone unpaired conditioning with lyral. In the right video, the mouse has undergone paired conditioning with lyral. Both videos are at 20X playback speed.

Movie S2.

Representative video of zone 1 of a cleared MOE from an M71-GFP$^{+/+}$ acetophenone unpaired mouse. M71 OSNs are visualized in white. Scale indicated in video.

Movie S3.

Representative video zooming into a nasal turbinate (zone 1) of a cleared MOE from an M71-GFP$^{+/+}$ acetophenone unpaired mouse. M71 OSNs are visualized in white. Scale indicated in video.

Movie S4.

Representative video of a cleared MOE from an M71-GFP$^{+/+}$ acetophenone unpaired mouse, showing coronal slices of a section of zone 1 from anterior to posterior. The top of the video is dorsal, and the bottom is ventral. Scale indicated in video.

Movie S5.

Representative video of zone 1 of a cleared MOE from an M71-GFP$^{+/+}$ acetophenone paired mouse. M71 OSNs are visualized in white. Scale indicated in video.

Movie S6.

Representative video zooming into a nasal turbinate (zone 1) of a cleared MOE from an M71-GFP$^{+/+}$ acetophenone paired mouse. M71 OSNs are visualized in white. Scale indicated in video.

Movie S7.

Representative video of a cleared MOE from an M71-GFP$^{+/+}$ acetophenone paired mouse, showing coronal slices of a section of zone 1 from anterior to posterior. The top of the video is dorsal, and the bottom is ventral. Scale indicated in video.